Muscle satellite cells are functionally impaired in myasthenia gravis: consequences on muscle regeneration

Mohamed Attia, Marie Maurer, Marieke Robinet, Fabien Le Grand, Elie Fadel, Rozen Le Panse, Gillian Butler-Browne, Sonia Berrih-Aknin

Muscle satellite cells are functionally impaired in myasthenia gravis: consequences on muscle regeneration

Mohamed Attia[1,2,3] · Marie Maurer[1,2,3] · Marieke Robinet[1,2,3] · Fabien Le Grand[1,2,3] · Elie Fadel[4] · Rozen Le Panse[1,2,3] · Gillian Butler-Browne[1,2,3] · Sonia Berrih-Aknin[1,2,3]

[1]Sorbonne universités, UPMC Université Paris 6, Paris, France, [2]INSERM U974, Paris, France, [3]AIM, Institut de Myologie GH Pitié-Salpêtrière, Paris, France, [4]INSERM U999, Centre Chirurgical Marie Lannelongue, Le Plessis-Robinson, France
Corresponding author: Sonia Berrih-Aknin, DSc, Phone: +33140778128, Fax: +33140778129, Electronic address: sonia.berrih-aknin@upmc.fr

Abstract

Myasthenia gravis (MG) is a neuromuscular disease caused in most cases by anti-acetyl-choline receptor (AChR) autoantibodies that impair neuromuscular signal transmission and affect skeletal muscle homeostasis. Myogenesis is carried out by muscle stem cells called satellite cells (SCs). However, myogenesis in MG had never been explored. The aim of this study was to characterise the functional properties of myasthenic SCs as well as their abilities in muscle regeneration. SCs were isolated from muscle biopsies of MG patients and age-matched controls. We first showed that the number of Pax7+ SCs was increased in muscle sections from MG and its experimental autoimmune myasthenia gravis (EAMG) mouse model. Myoblasts isolated from MG muscles proliferate and differentiate more actively than myoblasts from control muscles. MyoD and MyoG were expressed at a higher level in MG myoblasts as well as in MG muscle biopsies compared to controls. We found that treatment of control myoblasts with MG sera or monoclonal anti-AChR antibodies increased the differentiation and MyoG mRNA expression compared to control sera. To investigate the functional ability of SCs from MG muscle to regenerate, we induced muscle regeneration using acute cardiotoxin injury in the EAMG mouse model. We observed a delay in maturation evidenced by a decrease in fibre size and MyoG mRNA expression as well as an increase in fibre number and embryonic myosin heavy-chain mRNA expression. These findings demonstrate for the first time the altered function of SCs from MG compared to control muscles. These alterations could be due to the anti-AChR antibodies via the modulation of myogenic markers resulting in muscle regeneration impairment. In conclusion, the autoimmune attack in MG appears to have unsuspected pathogenic effects on SCs and muscle regeneration, with potential consequences on myogenic signalling pathways,and subsequently on clinical outcome, especially in the case of muscle stress.

Keywords: MG patients, AChR antibodies, Myogenic factors, Experimental autoimmune myasthenia gravis (EAMG)

Introduction

Myasthenia gravis (MG) is an autoimmune disease that affects the neuromuscular junction (NMJ). MG is caused by circulating autoantibodies against components of the post-synaptic membrane. In about 85% of cases, the autoantibodies target the nicotinic acetyl-choline receptor (AChR) [5, 15]. However, other targets, such as MuscleSpecific Kinase (MuSK) or Lipoprotein-Related Protein 4 (LRP-4), have been described [30, 58, 82]. In this study, we focused on the main form of the disease mediated by antiAChR antibodies. Although causes of the disease remain unclear, the immunopathogenic mechanisms are already established. The thymus appears to play a key role in the immune system dysregulation in the early form of the disease. It contains ectopic germinal centres including B cells synthesising anti-AChR antibodies [6]. The mechanisms of action of anti-AChR antibodies at the NMJ involve complement-dependent lysis of the post-synaptic membrane, receptor internalisation as well as direct interference with binding of acetylcholine to AChR [20, 31]. These alterations impair the neuromuscular transmission of the signal [57, 67] and thus could affect the function of the skeletal muscle fibres [41, 44]. Few studies describe the effects of the anti-AChR antibodies on muscle physiology and biology. For example, Zouvelou et al. reported, with magnetic resonance imaging, a human case of general muscle atrophy early in the disease before receiving steroid treatment [83]. Similarly, Martignago et al. have shown MG muscle fibre atrophy both in type I and type II fibres

but with a higher rate in type II fibres [41]. Maurer et al. revealed that anti-AChR antibodies alter IL-6 production in MG muscles affecting Akt/mTOR signalling pathways which could explain the observed muscle fatigability in MG [42]. PoëaGuyon et al. showed that MG-produced proinflammatory cytokines are able to up-regulate the expression of the adult AChR in muscles of EAMG mice [59]. Similarly, Guyon et al. demonstrated that anti-AChR antibodies are involved in the up-regulation of adult AChR mRNA expression in both the TE671 human rhabdomyosarcoma cell line and control human myotubes [28]. This last finding suggests the presence of a compensatory mechanism after the autoimmune attack regulating the expression of AChR in MG patients. It is noteworthy to mention that overexpression of AChR mRNA is observed in several other situations, such as the blockade of neuromuscular transmission and during denervation processes [28, 35].

Most physiological dysfunctions affect skeletal muscle homoeostasis and lead to the muscle repair that is carried out by two key steps: the activation and proliferation of musclespecific stem cells called satellite cells (SCs), and subsequent myogenic differentiation and maturation of the regenerated muscles. SCs are located between the sarcolemma and basement membrane of the muscle fibres [43]. They are the main cell-type controlling postnatal skeletal muscle growth and repair [13, 51]. The crucial role of SCs in regenerating damaged muscle has been extensively described [37, 61]. When SCs switch from a quiescent to an activated state, they become myoblasts. They are able to proliferate both in vivo in regenerating muscle and in vitro in high serum-containing medium, expressing myogenic factors such as MyoD and MyoG. These factors play an essential role in the proliferation and differentiation of SCs, respectively [81]. In normal physiological conditions, most SCs are maintained in a quiescent undifferentiated state in the muscle and express the specific Pax7 marker [65]. However, myopathies, injuries, or intense effort that could represent a muscle stress rapidly activate SCs to form new myofibres and repair damaged muscle [37].

Although the muscle is the target organ, molecular and cellular mechanisms of myogenesis in MG are still unknown. The aim of this study was to investigate whether SCs from MG muscle display functional differences compared to those from control muscles. To reach this goal, we analysed the proliferation and differentiation capacity of SCs isolated from human control and MG muscles. In addition, we studied muscle regeneration following toxin injury in the experimental mouse model of myasthenia gravis (EAMG). We showed that SCs from MG muscles displayed higher rates of proliferation and differentiated more than SCs from control muscles. The treatment of control human myoblasts with MG sera or anti-AChR monoclonal antibodies increased differentiation via modulation of the myogenic factor MyoG. We found that regenerated muscle in EAMG mice displayed smaller fibres with higher mRNA expression of MyoG and embryonic myosin heavy chain (MyHC) compared to control mice. To conclude, our results demonstrate for the first time that the autoimmune attack by the anti-AChR antibodies in MG results in substantial functional changes of the SCs, with potential consequences on the clinical outcome.

Materials and methods

Experimental autoimmune myasthenia gravis (EAMG) induction

The EAMG induction was performed as previously described [70] with some modifications to optimize the rate of sick animals [78]. Five-week-old female C57Bl/6J mice were obtained from Janvier laboratories (Le Genest SaintIsle, France) and acclimatized 1 week in the SPF animal facility (CEF, Université Pierre et Marie Curie) prior to the immunization procedure. The experiments were performed following the principles of the French council on animal care (authorisation number: 02637). AChR was extracted and purified from the electric organ of *Torpedo californica* by chromatography as previously described [1]. To induce EAMG, the mice (n = 13) were immunized by five subcutaneous injections, two in both hind footpads and three in the back, with *Torpedo* AChR (30 µg/mouse) emulsified in Complete Freund Adjuvant (CFA) further supplemented with non-viable *Mycobacterium tuberculosis* (1 mg/mouse). Control (Ctl) mice (n = 6) were immunized only with CFA further supplemented with non-viable *Mycobacterium tuberculosis* at the same concentration. Four weeks later, a boost was performed with one injection in the back using the same amount of *Torpedo* AChR in CFA. The control mice received only CFA. Grip strength and the weight of the mice were monitored every 2 weeks and the global clinical score was calculated taking into account the loss of weight, the grip test, and the grid test as fully described in Weiss et al. [78]. Each test had a maximum score of 3, and then, the maximum clinical score was 9. The mice were considered sick when their global clinical score reached 2 or higher. Ten mice out of 14 were sick in this experiment, which means 71% of the total mice. We did not evaluate the AChR antibody level, as this level is generally high in the immunized mice but not correlated with the clinical status [78].

Cardiotoxin-induced muscle regeneration

When the percentage of sick mice (score ≥2) reached 70% (Online Resource Fig. S1a), acute skeletal muscle regeneration was performed as described in [16] and reviewed in [24]. Briefly, 30 µl of cardiotoxin at the concentration of 12 µM in saline (Latoxan, Portes-lès-Valence, France) was injected into *tibialis anterior* (TA) muscles to induce muscle injury and subsequent regeneration. Control and EAMG right TA muscles were injected with cardiotoxin to induce regeneration, while the contralateral TA muscles from the same mice were injected with PBS. Mice were sacrificed by progressive CO_2 inhalation 7 days after injection and TA were collected, snap frozen in N_2-precooled isopentane, and stored at −80 °C until use. We choose the 7 days window as the satellite cells are activated at this step [24].

Human muscle biopsies

Human muscle biopsies (Online Resource Tables S1a and S1b) were obtained from MG patients (n = 20) and age-matched controls (n = 19) (20–56 years) undergoing thymectomy or cardiovascular surgery, respectively. Since the age, but not the gender, can affect the quality of the skeletal muscle and the quantity of SCs [53], the control muscles were agebut not sex-matched. Biopsies were derived from the *pectoralis major* muscle under sterile conditions and in accordance with the declaration of Helsinki and approved by French committee on ethical rules "Comité de Protection des Personnes (CPP, Ile-de-France VI)", GH Pitié-Salpêtrière, Paris, France (authorization number 2010-A00250-39). All participants gave informed written consent to use their biopsies. For histological analysis, muscles (Ctl n = 5, MG n = 5) were aligned, frozen in N_2-precooled isopentane, and stored at -80 °C until use. For total RNA isolation, muscles (Ctl n = 9, MG n = 10) were put into cryotubes under sterile conditions, frozen in liquid N_2 until use. For SC isolation, another batch of muscle specimens (Ctl n = 6, MG n = 6) was used.

Human primary myoblast cultures

SCs were isolated from muscle biopsies using the explant method as previously described [21]. Note that once SCs migrate out from the muscle explant, they became active and they are called myoblasts. Briefly, biopsies were rinsed in Phosphate Buffered Saline (PBS) supplemented with antibiotics (penicillin 100 units/ml, streptomycin100 µg/ml) then scissor-minced in Foetal Bovine Serum (FBS, Eurobio, Les Ulis, France). The tissue fragments were plated into 75 cm^2 flasks (BD Biosciences, Le Pont de Claix, France) pre-coated with 0.2% gelatin (SigmaAldrich, Saint-Quentin Fallavier, France). After 10 days of culture in growth medium (GM) containing four parts Dulbecco's modified Eagle's medium (DMEM, 4.5 mg/ ml glucose, Life Technologies, Saint Aubin, France), one part medium 199 (Life Technologies), 20% FBS (Eurobio), 5 µg/ml bovine insulin (Sigma-Aldrich), 0.5 ng/ml fibroblast growth factor (Life Technologies), 5 ng/ml epidermal growth factor (Life Technologies), 0.2 µg/ml dexamethasone (Life Technologies), and 50 µg/ml fetuin (Life Technologies); the cells which had migrated out of the explants were trypsinized and collected by centrifugation. The myoblasts were then positively selected using anti-CD56 magnetic microbeads according to the manufacturer's instructions (Miltenyi Biotec, Bergisch Gladbach, Germany). CD56 positive cells, which represent generally about 90–95% of total cells after cell sorting, were incubated in 75 cm^2 flask at 37 °C in a humid atmosphere containing 5% CO_2 then expanded in GM. Since the intermediate filament protein desmin is muscle specific, the myogenic purity of the cell culture was monitored using desmin immunolabeling by counting the number of desmin-positive cells as a percentage of the total number of nuclei. The primary myoblast cultures were considered to be pure enough to be used for our experiments when their percentage in the culture was 90% or more.

Myoblast proliferation assay

Proliferation of myoblasts was assessed using a flow cytometry counting tool. Briefly, after expansion of the CD56 positive myoblasts, control and MG myoblasts were seeded into six-well plates (BD Biosciences) at 2000 cells/cm^2 in GM. After 1–4 days of proliferation, the cells were trypsinized, washed, and fixed with 4% paraformaldehyde, then analysed on a FACSVerse Flow cytometer for counting with Flow Sensor tool (BD Bioscience). Cell density was normalized to the volume used to count.

Myoblast differentiation assay

The differentiation was assessed by fusion index and myotube size using MF20 antibody (Hybridoma Bank DSHB, Iowa City, IA, USA) which labels muscle Myosin Heavy Chain (MyHC). MyHC is a specific marker of differentiated fibres. Fusion index was calculated as the ratio of the number of nuclei into myotubes to the total number of nuclei. Myotube size was evaluated as the stained surface of MF20 using the ImageJ analysis software [60]. Briefly, myoblasts were seeded on to sixwell plates (BD Biosciences) at 50,000 cells/cm^2 in GM as described above. The day after, when cells stuck to the plates, GM was shifted to differentiation medium (DM) containing DMEM 4.5 mg/ml glucose, 5 µg/ml bovine insulin (Sigma-Aldr ich), and 0.1% Ultroser-G (w/v)(Sigma-Aldrich). Then, the cultures were supplemented or not with control or MG patient sera. In some experiments, the cultures were supplemented with monoclonal antibodies against AChR (Kindly provided by Tzartos et al. [71]) or IgG2a isotype control (R&D Systems, Inc. Abingdon, United Kingdom) according to the experiments. The sera were used diluted at 1/100 in the DM. The monoclonal antibodies and their relevant isotype control were used at a final concentration of 3 µg/ml.

Histology and immunofluorescent labelling

Freshly frozen muscles were used for immunofluorescence. Cryostat sections (7 µm thick) of *tibialis anterior* and *pectoralis major*, respectively, from mice and humans were made, air-dried under the hood for 10 min, and fixed in 4% paraformaldehyde (w/v) for 20 min at room temperature (RT). Sections were then processed for antigen retrieval with unmasking solution (CliniSciences, Nanterre, France) at 95 °C for 15 min and blocked with PBS-BSA 5% (w/v) for 2 h then incubated overnight (ON) at 4 °C with antiPax7, anti-MyoD, anti-Ki67, and anti-laminin. Bound antibodies were revealed with the appropriate Alexa conjugated secondary antibodies (Fluoprobes Interchim, Montluçon, France). Antibodies are listed in Table 1. For MyHC labelling, myotubes at day 0, day 2, and day 4 of differentiation were washed with PBS and fixed with cold ethanol for 20 min at −20 °C. Then, cultures were blocked with PBS-BSA 5% (w/v) for 1 h and incubated ON at 4 °C with anti-MyHC monoclonal antibody (MF-20). Bound antibody was detected with appropriate AlexaFluor-488 conjugated secondary antibody (Fluoprobes, Interchim). Nuclei were counter-stained with DAPI (1 µg/ml) for 5 min at RT. For haematoxylin and eosin (H&E) staining, mouse TA sections were air-dried then fixed in 4% paraformaldehyde (w/v) for 10 min at RT. After washing twice in PBS, sections were stained with Mayer's haematoxylin for 10 min, washed in tap water and stained in eosin for 2 min. Sections were then dehydrated few seconds in progressive baths of ethanol, cleared twice in xylene for 15 min each, and finally mounted in permanent mounting medium (CliniSciences). For fusion index and myotube size quantification, approximately 2500 nuclei of total nuclei were counted by well and duplicate wells were analysed. For mouse muscles, approximately 1500 fibres were counted. For human muscles, approximately 800 fibres were counted. Images were acquired with the Zen software (Carl Zeiss, Marly le Roi, France) using Axiocam MRm CCD monochrome camera fitted to Axio Observer.A1 epifluorescence microscope (Carl Zeiss, Marly le Roi, France). Image analysis and quantification were performed using colour segmentation procedure programmed with ImageJ [60].

mRNA isolation and quantitative PCR (qPCR)

Total RNA was extracted from mouse *tibialis anterior*, human *pectoralis major* and human myoblasts and myotubes with Trizol reagent (Life Technologies) according to the manufacturer's instructions. The sample concentration and purity was assessed using the NanoDrop spectrophotometer. cDNA synthesis was performed on 1 µg of total mRNA extracts for 1 h at 42 °C using Oligo-dT primers and *Avian Myeloblastosis Virus* (AMV) reverse transcriptase (Life Technologies) in a final volume of 50 µl. One microliter of the resulting cDNA was submitted to SYBR Green qPCR amplification using a LightCycler® 480 system (Roche Life Sciences, Meylan, France), as previously described [38]. Primer sequences (Eurogentec, Angers, France) were designed using the online Primer3 software. The primer sequences and qPCR details are shown in supplemental data (Online Resource Table S2). For Ki67, primers were ready-to-use and provided from RealTimePrimers. com.

Statistical analysis

Data are expressed as mean ± SEM. Data shown are representative of two repeated experiments using the same samples in duplicate. Differences between groups were compared using the non-parametric Mann–Whitney test

using the GraphPad Prism 6 software (San Diego, CA, USA). For myofibre distribution analysis, differences between groups were compared with two-way ANOVA Bonferroni's multiple comparisons test. Significant differences were determined at $p < 0.001$ (***), $p < 0.01$ (**), and $p < 0.05$ (*).

Table 1 Information about primary and secondary antibodies

Molecular specificity	Species specificity	Species origin and IgG isotype	Clone	Dilution	Application	Manufacture
Primary antibodies						
Pax7	Mouse/Rat/Human	Mouse mAB IgGl	PAX7	1/10	IH	Hybridoma Bank DSHB, IA, USA
MyoD	Mouse/Rat/Human	Mouse mAB IgGl	5.8A	1/50	IH	BD Pharmingen, NJ, USA
MyHC	Human	Mouse mAB lgG2b	MF-20	1/20	IH	Hybridoma Bank DSHB; IA, USA
Ki67	Human	Rat mAB IgGl	5D7	1/100	IH	Abeam, Paris, France
CD56	Human	Mouse mAB IgGl		1/5	Sorting	Miltenyi Biotec, Bergisch Gladbach, Germany
Laminin	Mouse/Rat/Human	Rabbit pAB IgG		1/200	IH	Dako, Les Ulis, France
Secondary antibodies						
IgG	Mouse	Alexa-488goat polyclonal		1/400	IH	Fluoprobes Interchim, Montlucon, France
IgG	Rat	Alexa-488 donkey polyclonal		1/300	IH	Fluoprobes Interchim, Montlucon, France
IgG	Mouse	Alexa-555goat polyclonal		1/300	IH	Fluoprobes Interchim, Montlucon, France
IgG	Rabbit	Alexa-488 donkey polyclonal		1/400	IH	Fluoprobes Interchim, Montlucon, France
IgG	Mouse	AffiniPureFab Fragment goat		1/50	IH	Jackson Immunoresearch, PA, USA

IH immunohistology, *IgG* immunoglobulin G, *mAB* monoclonal antibody, *pAB* polyclonal antibody

Results

SC number was increased in mouse EAMG and human MG skeletal muscle

To analyse whether the SCs were affected in MG, *TA* muscles were collected from control and EAMG mice and were submitted to Pax7 immunolabeling and RT-qPCR. Pax7 is a specific marker of SCs [65]. We showed that the number of Pax7+ SCs (in red), localised between the sarcolemma and the basal lamina characterised by laminin staining (in green) (Fig. 1a, b) was increased in the TA of EAMG muscles compared to controls (Fig. 1c). The significantly high mRNA expression of Pax7 in EAMG muscles (Fig. 1d) evaluated by RT-qPCR confirmed that AChR-injected mice displayed more SCs than CFAinjected mice in their skeletal muscle after 7 weeks of immunization. Then, to investigate whether human MG muscle displayed similar alteration as in EAMG mice, we performed quantitative analysis of Pax7 using immunolabeling and RT-PCR. We observed that MG muscles displayed significantly more SCs than controls (Fig. 2a–c). This result was confirmed by a higher mRNA expression of Pax7 in MG muscle biopsies compared to the controls (Fig. 2d). These results suggest that the myogenic cell population is affected in MG.

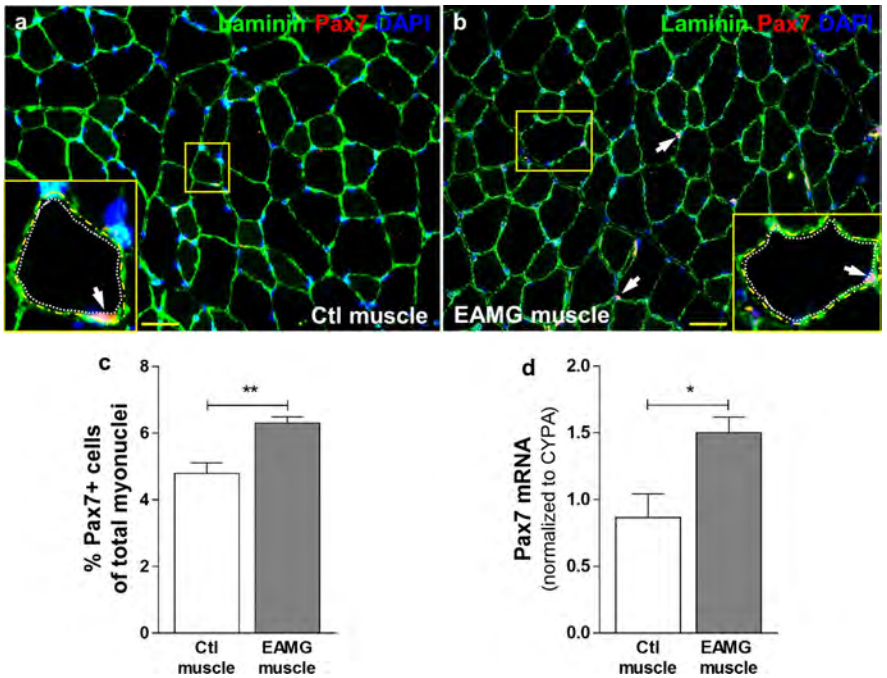

Fig. 1 EAMG mice displayed more satellite cells in their *tibialis anterior* muscles than control ones. Pax7 immunolabeling (**a**, **b**), quantification of Pax7+ nuclei (**c**), and Pax7 mRNA expression (**d**) in Ctl ($n = 6$) and EAMG ($n = 6$) mouse *TA* muscles. Pax7 is a specific marker of SCs. *Yellow squares* show magnification of one transversal myofibre section containing SCs. *White arrows* show SCs which are located between basal lamina (*yellow dotted line*) and sarcolemma (*white dotted line*). Pax7+ nuclei quantification was normalized to the total number of myonuclei. Nuclei were stained with DAPI. Cyclophilin A (CYPA) was used as an internal control for qPCR. Values represent the mean ± SEM. $p < 0.05$ (*), $p < 0.01$ (**). *Bar* 20 µm

SCs of human MG skeletal muscles displayed high proliferative rate

Since we found more SCs in human MG skeletal muscles compared to control ones, we next asked whether the SCs in MG muscles were active and functional. To this end, we analysed the expression of MyoD and Ki67, two markers of SC activation and proliferation, on muscle sections. The co-immunolabeling of Pax-7 and laminin identified the SCs (Fig. 3a), and the co-immunolabeling of MyoD and laminin in serial sections (Fig. 3b) allowed us to investigate whether the Pax-7+ cells were activated. In parallel, the co-immunolabeling of Pax7 and Ki67 showed the SCs (Pax7+ cells) that were in proliferating state (Ki67+ cells) (Fig. 3c). The precise counting of the positive cells demonstrated that MG muscles displayed a significantly higher number of MyoD and Ki67 positive cells among

total SCs (respectively, Fig. 3d, f) compared with controls. This was confirmed by the higher mRNA expression of MyoD and Ki67 in MG muscle biopsies compared to the controls (respectively, Fig. 3e, g). Together, these results suggest that SCs were more active in MG muscles and displayed higher proliferative rate during MG disease compared to control muscles.

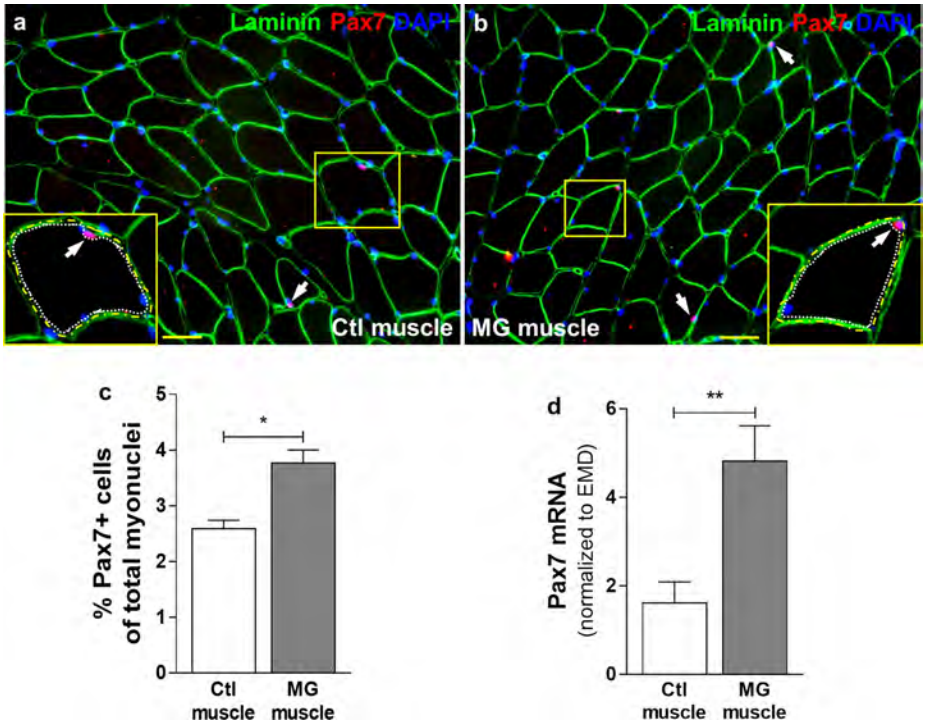

Fig. 2 Human MG muscles displayed more satellite cells than control ones. Pax7 immunolabeling (**a**, **b**), quantification of Pax7+ nuclei (Ctl $n = 5$, MG $n = 5$) (**c**), and Pax7 mRNA expression (Ctl $n = 9$, MG $n = 10$) (**d**) in Ctl and MG human muscle biopsies. It should be noted that patients with thymoma behave similarly as non-thymoma patients. *Yellow squares* show magnification of one transversalmyofibre section containing SCs. *White arrows* show SCs which are located between basal lamina (*yellow dotted line*) and sarcolemma (*white dotted line*). Pax7+ nuclei quantification was normalized to the total number of myonuclei. Nuclei were stained with DAPI. Emerin (EMD) was used as an internal control for qPCR. Values represent the mean ± SEM. $p < 0.05$ (*), $p < 0.01$ (**). *Bar* 20 μm

Isolated human MG myoblasts proliferate more actively than control ones

We then explored the functional features of the SCs isolated from MG and control biopsies. As mentioned above, once SCs move out from their muscle environment, they became active, and they are called myoblasts. Myoblasts were cultured in high serum-containing medium during
4 days (Fig. 4a, b). Cells were counted every day using the FACSVerse Flow Sensor counting tool. We showed that myoblasts from MG muscles proliferated more actively than control cells at day 3 and day 4 (Fig. 4c). Using RTqPCR, we observed that mRNA expression of Myf5, the myoblast activation marker, was gradually decreased during proliferation similarly in MG and control myoblasts (Fig. 4d). mRNA expression of MyoD, the myogenic proliferation marker, was gradually increased during proliferation in MG and control myoblasts, but to a greater extent in MG myoblasts (Fig. 4e). mRNA expression of Ki67 was gradually increased up to day 3 and then decreased at day 4 of proliferation. However, at day 3, Ki67 mRNA was significantly increased in MG myoblasts compared to controls (Fig. 4f). These results show that control and MG myoblasts displayed biologically different features even out of their muscle environment. The increase mRNA MyoD expression in MG myoblasts suggests its implication for the observed high proliferation.

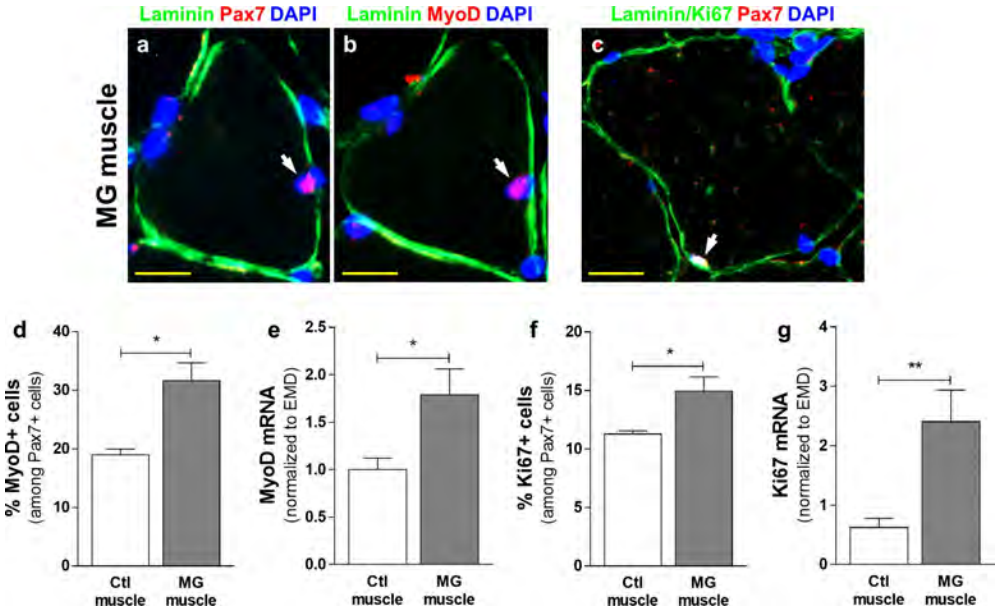

Fig. 3 Human MG muscles displayed satellite cells with higher proliferative rate than control ones. Pax7 (**a**, **c**), MyoD (**b**), and Ki67 (**c**) immunolabeling, quantification of MyoD+ and Ki67+ cells (Ctl $n = 5$, MG $n = 5$) (respectively, **d** and **f**) among Pax7+ cells, and MyoD and Ki67 mRNA expression (Ctl $n = 9$, MG $n = 10$) (respectively, **e** and **g**) in Ctl and MG human muscle biopsies. It should benoted that patients with thymoma behave similarly as non-thymoma patients. Serial sections were used for Pax7 and MyoD immunolabeling in (**a**) and (**b**). White arrows show Pax7+ (**a**), MyoD+ (**b**), or Pax7+/Ki67+ (**c**) cells. Nuclei were stained with DAPI. Emerin (EMD) was used as an internal control for qPCR. Values represent the mean ± SEM. $p < 0.01$ (**), $p < 0.05$ (*). *Bar* 5 µm

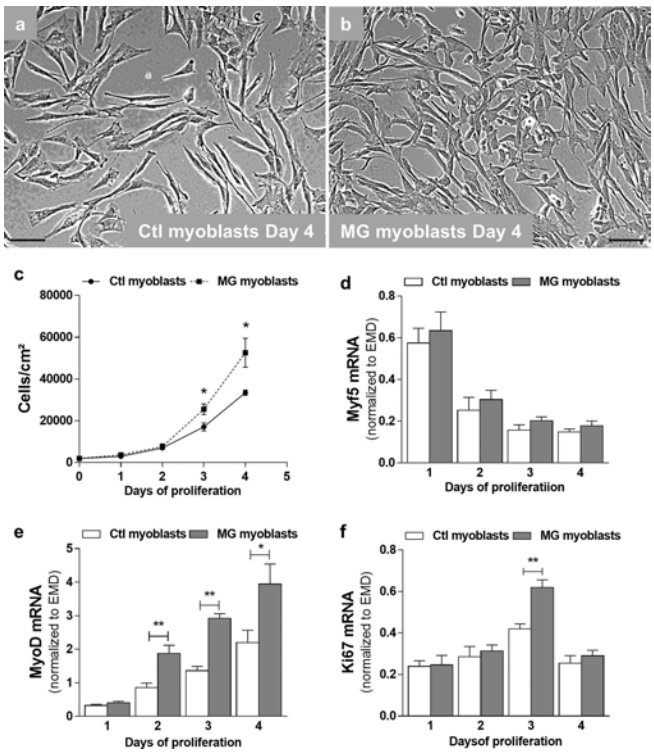

Fig. 4 Myoblasts from MG muscle biopsies proliferated faster than those from control ones. Myoblasts, which are isolated and activated SCs, from Ctl ($n = 6$) and MG ($n = 6$) muscle biopsies were allowed to proliferate in kinetic study (day 0–day 4) in growth medium. Phase-contrast microscopy views (**a**, **b**), cell density quantification(**c**), and Myf5 (**d**), MyoD (**e**), and Ki67 (**f**) mRNA expression of Ctl and MG myoblasts during proliferation. Emerin (EMD) was used as an internal control for qPCR. Values represent the mean ± SEM. $p < 0.05$ (*), $p < 0.01$ (**). *Bar* 50 µm

Human MG myoblasts differentiated more rapidly than control ones

To investigate further the functional differences between SCs from MG and control biopsies, we examined the differentiation of these myoblasts. By shifting the cell culture to serum-free medium, human myoblasts differentiate and fuse into multinucleated myotubes [54, 79]. To evaluate cell differentiation, we calculated fusion index and myotube size in cultures stained with anti-myosin heavy-chain (MyHC) antibody (MF20) which is a specific antibody to label myotubes. Staining of control and MG myotubes are shown in Fig. 5a, b, respectively. We demonstrated that myoblasts from MG muscles displayed higher fusion index and bigger myotubes than myoblasts from control ones at day 2 and day 4 of differentiation (respectively, Fig. 5c, d). These results suggest that MG myoblasts differentiate more rapidly than control ones. These findings were confirmed by mRNA expression investigation. Indeed, the specific marker of differentiation, MyoG, was expressed at a higher level in MG myotubes compared to controls at day 4 of differentiation (Fig. 5e). Moreover, similar to cultured myotubes, MG muscles biopsies displayed higher MyoG mRNA expression compared to control muscle biopsies (Fig. 5f). These results suggest that cultured myoblasts from MG and control muscles showed biological differences and that MG myoblasts exhibited specific features that could explain the observed increased differentiation.

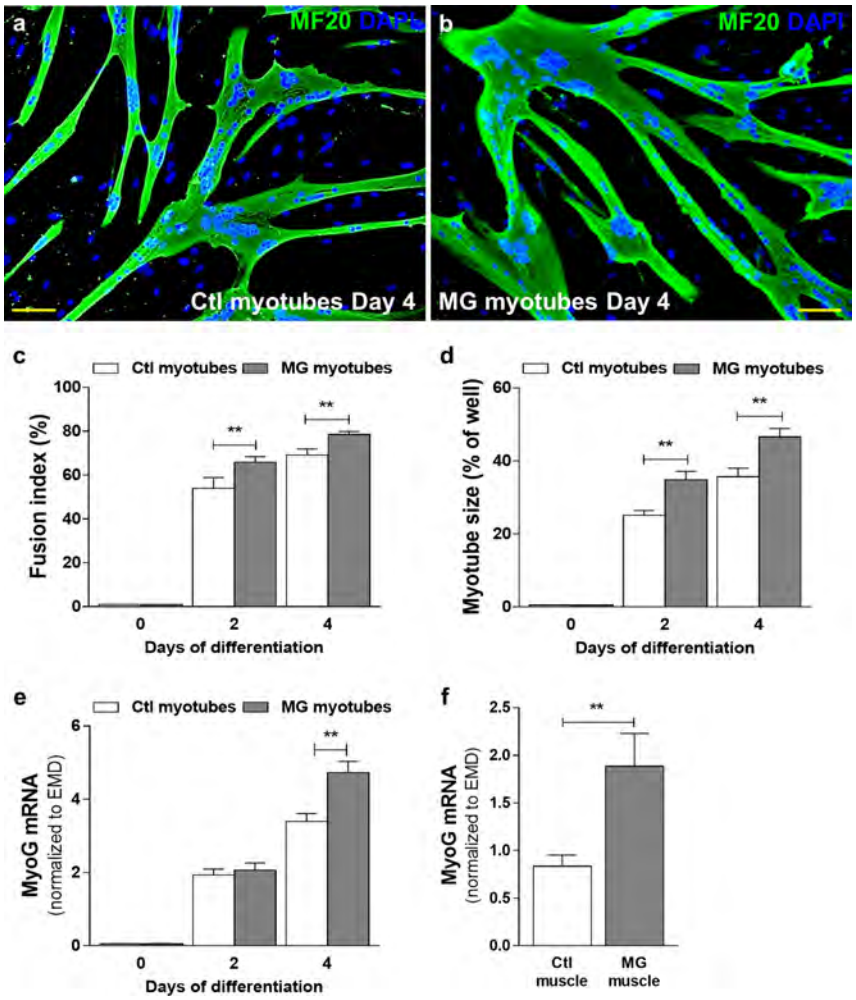

Fig. 5 Myoblasts from MG muscles differentiate more than those from control ones. Myoblasts from Ctl (n = 6) and MG (n = 6) muscle biopsies were allowed to differentiate in kinetic study (day 0–day 4) in differentiation medium forming myotubes. MF20 immunolabeling of Ctl (**a**) and MG (**b**) myotubes at day 4 of differentiation. MF20 label total muscle Myosin Heavy Chain (MyHC). Differentiation was evaluated by fusion index (**c**) and myotube size (**d**), as described in "Materials and methods. MyoG mRNA expression was measured during differentiation (**e**) as well as in control and MG muscle biopsies (Ctl n = 9, MG n = 10) (**f**). It should be noted that patients with thymoma behave similarly as non-thymoma patients. Nuclei were stained with DAPI. Emerin (EMD) was used as an internal control for qPCR. Values represent the mean ± SEM. $p < 0.01$ (**). *Bar* 50 µm

Sera of MG patients increased differentiation of control myoblasts

To investigate the functional properties of the myoblasts in MG conditions, with the aim to define factors that were responsible for the observed high proliferation and differentiation, we analysed the effects of sera from MG patients on the proliferation and differentiation of human control myoblasts. MG sera treatment had no effect on proliferation (Online Resource Fig. S3a, S3b, and S3c) neither on MyoD mRNA expression (Online Resource Fig. S3d) compared to control sera. However, in the differentiation assay, we showed that MG sera treatment significantly increased the differentiation of control myoblasts (Fig. 6a, b) assessed by the high fusion index (Fig. 6c) and the high myotube size (Fig. 6d) compared with control sera treatment at days 2 and 4. The high expression of MyoG mRNA at day 4 (Fig. 6e) confirmed the increased differentiation of the control myoblasts treated with MG sera compared with those treated with control sera. These results suggest that the MG serum contains one or more factors responsible for the increase differentiation observed in control myoblasts.

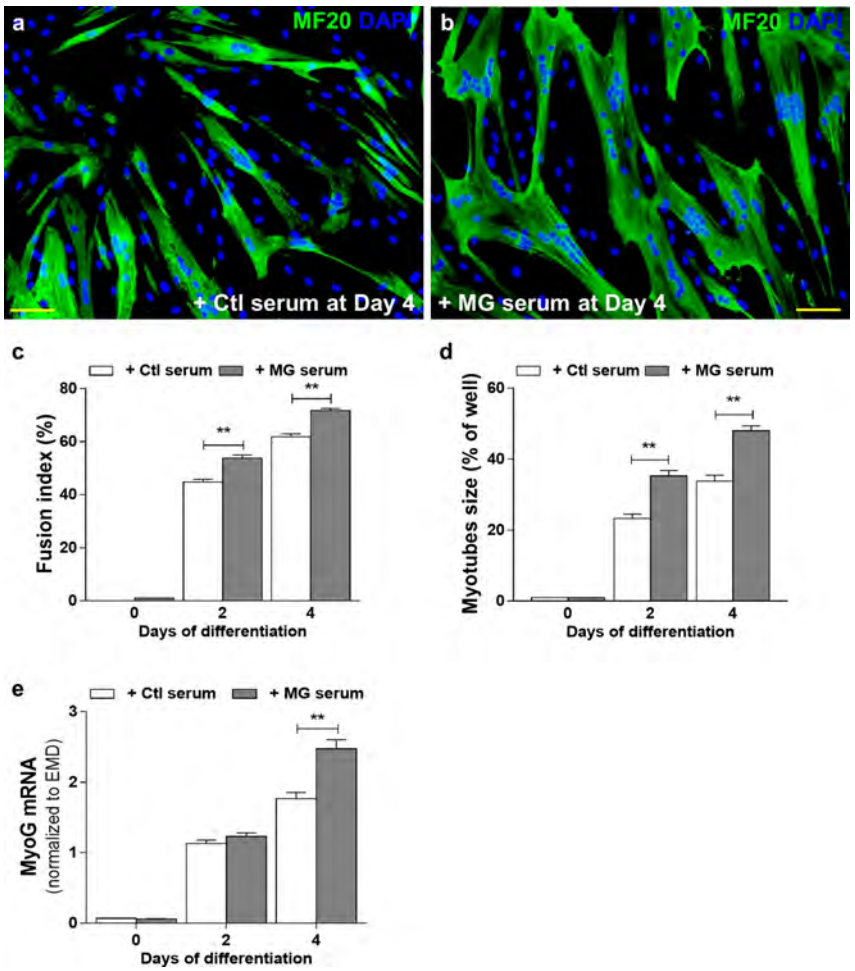

Fig. 6 Control myoblasts treated with MG sera differentiated more than those treated with control sera. Myoblasts from control muscle biopsies (n = 6) were allowed to differentiate in kinetic study (day 0–day 4) in differentiation medium supplemented with Ctl (n = 3) or MG (n = 6) sera. MF20 immunolabeling of control myotubes at day 4 of differentiation treated with Ctl (**a**) or MG (**b**) sera. Differentiationwas evaluated by index fusion (**c**) and myotube size (**d**), as described in "Materials and methods". MyoG mRNA expression (**e**) was measured during the differentiation. Emerin (EMD) was used as an internal control for qPCR. Values represent the mean ± SEM. $p < 0.01$ (**). *Bar* 50 µm

Monoclonal anti-AChR antibodies induce an increased differentiation of control myoblasts

Since one main difference between MG and control serum is the presence of the antibodies against AChR, we investigated whether the high differentiation observed in MG myoblasts could be due to the pathogenic effect of anti-AChR antibodies. To answer this question, we tested two different anti-AChR monoclonal antibodies (198 and 155) and their relevant isotype as control (IgG2a). The mAB198 antibody is directed against the main extracellular immunogenic region of the alpha subunit of AChR, whereas mAB155 antibody binds to its major epitope of the cytoplasmic side [71]. We observed that both mAB198 and mAB155 antibodies had a significantly larger effect compared to IgG2a isotype control (Fig. 7a–c) on fusion index (Fig. 7d) and myotube size (Fig. 7e) exhibiting a better differentiation of control myoblasts at days 2 and 4. The effect of antiAChR antibodies on control myoblast differentiation was confirmed by high MyoG mRNA expression at days 2 and 4 for mAB155 antibody but only at day 4 for mAB198 antibody (Fig. 7f). Since MG sera and purified monoclonal anti-AChR antibodies had similar effects on control myoblasts, these data suggest that anti-AChR antibodies in MG sera were able to induce muscle differentiation probably via modulation of MyoG expression.

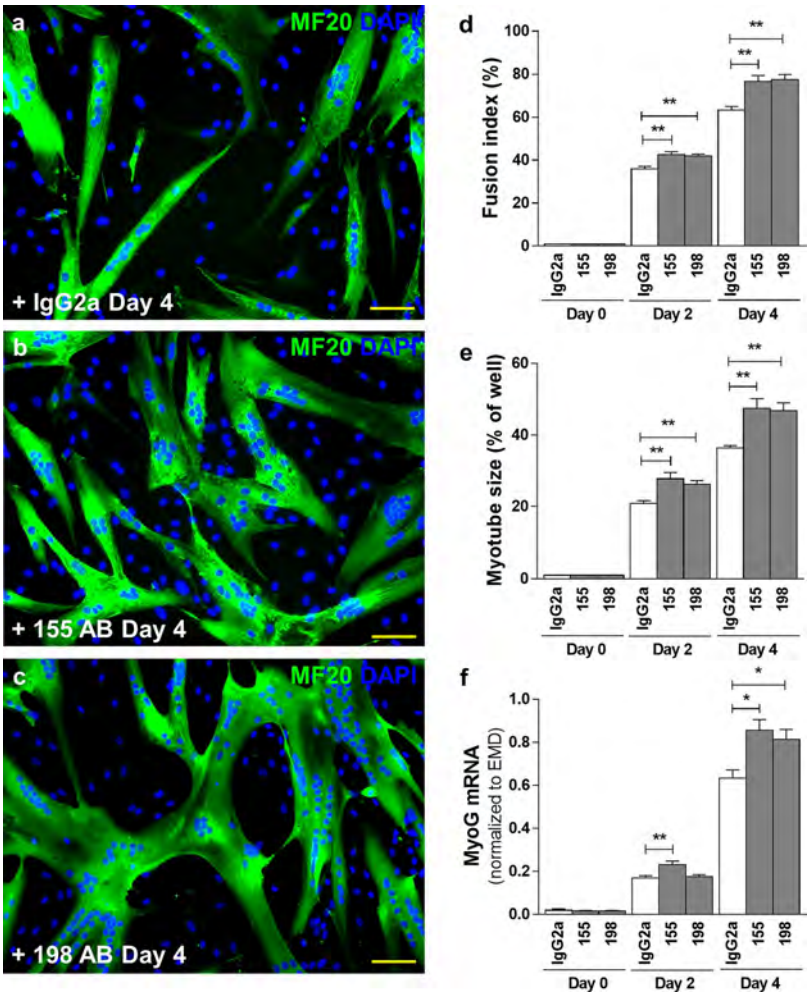

Fig. 7 Monoclonal anti-AChR antibodies induced higher differentiation of control myoblasts than IgG isotype. Myoblasts from control muscles ($n = 6$) were allowed to differentiate in kinetic study (day 0–day 4) in differentiation medium supplemented with two different monoclonal anti-AChR antibodies (155 and 198) and a relevant IgG isotype control (IgG2a). MF20 immunolabeling of control myotubes at day 4 of differentiation treated with Isotype control IgG2a (**a**) or 155 antibody (**b**) or 198 antibody (**c**). Differentiation was evalu-ated by fusion index (**d**) and myotube size (**e**), as described in "Materials and methods". MyoG mRNA expression (**f**) was measured during the differentiation. Emerin (EMD) was used as an internal control for qPCR. Values represent the mean ± SEM. $p < 0.05$ (*) and $p < 0.01$ (**). *Bar* 50 μm

Delayed muscle regeneration in myasthenic skeletal muscle following acute injury

Since our results showed that anti-AChR autoantibodies could be responsible for the alteration of SC features in vitro, we asked whether the main function of SCs, i.e., muscle regeneration, was altered in myasthenic muscles in vivo. To address this question, we induced EAMG in mice. The different clinical scores and clinical items (weight, grid score, and grip strength) are shown in Fig. S1 (Online Resource). Then, we injured right TA muscles (nominated R-muscle) in control and EAMG mice by cardiotoxin injection (see experimental design in Fig. 8a), while the contralateral TA muscles from the same mice were injected with PBS. We analysed the morphology and distribution of muscle fibres at day 7 of regeneration. Figure S6 shows the efficiency of the muscle regeneration in non-EAMG mice: the CSA mean is reduced and MyoG is increased in the cardiotoxin injected-muscle compared to contralateral muscle of the same mice (Online Resource Fig. S6). In addition, in the Ctl muscle, we did not observe significant differences in the size and number of fibres compared to EAMG muscle, indicating that in the absence of muscle injury (Online Resource Fig. S4 and Fig. S5), there is no sign of altered regeneration in the myasthenic muscle. Similar features were observed in human muscle biopsies that did not display significant muscle atrophy or features of ongoing regeneration process (not shown).
We then compared the R-muscle in control and EAMG mice. First and as expected, we observed that in both groups of mice, the R-muscles displayed many centrally nucleated myofibres (Fig. 8b) that represent newly regenerated fibres. However, regenerated EAMG muscles significantly showed smaller cross-sectional area (CSA) (Fig. 8c), and a higher number of fibres (Fig. 8d) compared to the control ones. A detailed analysis of the muscle section areas revealed that EAMG muscles exhibited a large number of fibres with a CSA lower than 550 μm^2 compared to control muscles (Fig. 8e). Furthermore, we showed that the CSA, the number, and the distribution of the size of the myofibres in EAMG muscles were correlated with the clinical score of the mice (respectively, Fig. 8f–h), suggesting a direct relationship between the severity of the EAMG and its effect on regenerated muscles. Similar results were obtained when the classical clinical scale was used (Online Resource Fig. S2), although the results were less striking, likely because the classical clinical scale includes only five scoring levels (0–4) instead of ten in our global clinical score (0–9).

To further investigate the mechanisms involved in muscle regeneration of EAMG mice, we analysed the expression of myogenic markers in the muscle. We showed that Pax7 mRNA expression (Fig. 9a) was not significantly different in EAMG and control muscles at day 7 of regeneration. However, we observed a significant decrease in MyoG mRNA expression (Fig. 9b) and an increase in the embryonic MyHC mRNA expression (Fig. 9c) in EAMG muscles compared to the control ones. Moreover, we showed that the embryonic MyHC mRNA expression in EAMG muscles was correlated with the clinical score of the mice (Fig. 9d). Taken together, these results suggest that the alteration of the muscle repair in EAMG mice could result from the impairment of the fusion and maturation processes of newly formed fibres during the muscle regeneration.

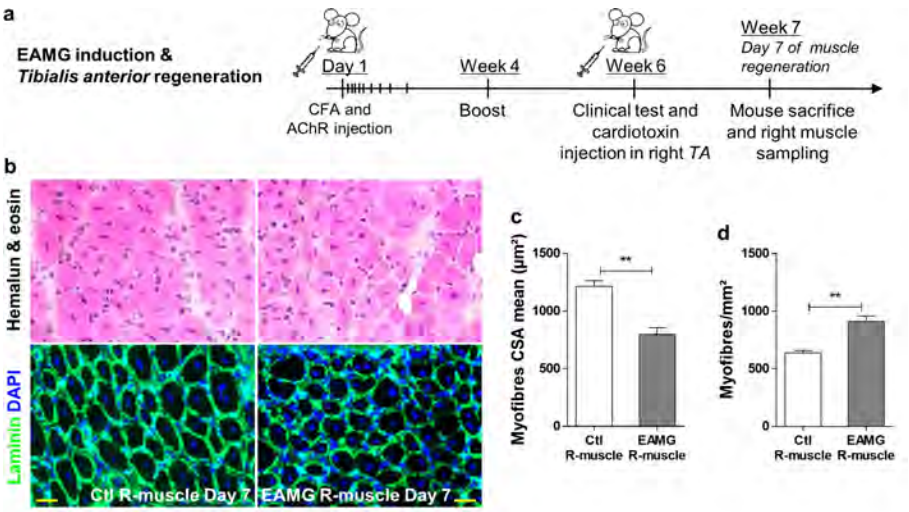

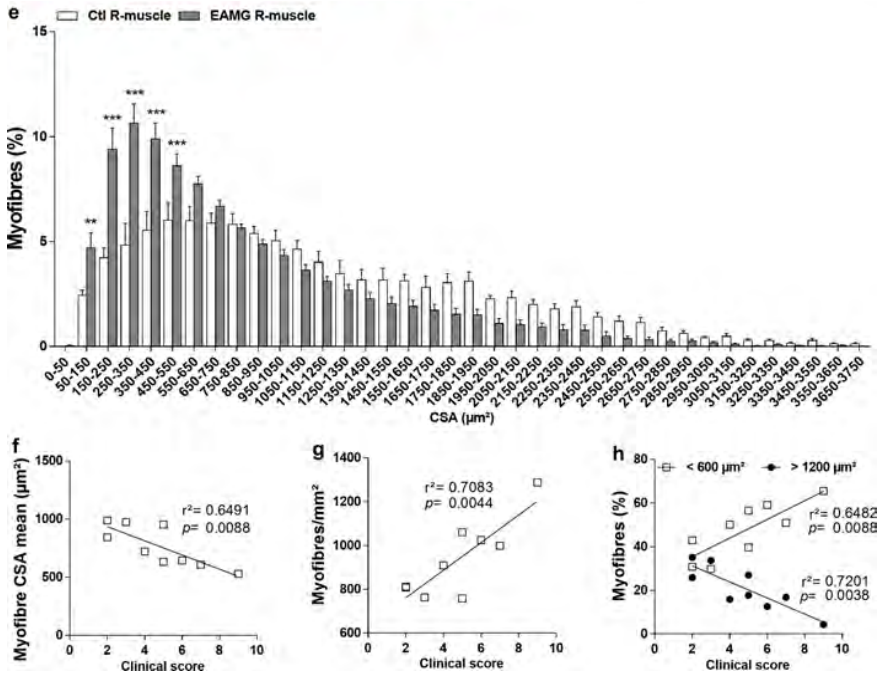

Fig. 8 EAMG regenerated muscle displayed more and smaller fibres than control regenerated ones following an acute injury. Experimental design (**a**): 6-week-old female randomised-mice were injected subcutaneously at day 1 with CFA (n = 6) or CFA+AChR (n = 13) to induce experimental autoimmune myasthenia gravis (EAMG). At week 6, when the global clinical score of EAMG mice reached at least 2, control and EAMG right TA muscles (R-muscle) were injected with cardiotoxin to induce regeneration. Left TA muscles were used as contralateral. At day 7 post-cardiotoxin injections, muscles were sampled then analysed. Haematoxylin and eosin staining (**b**, *upper panels*) and Laminin immunolabeling (**b**, *bottom panels*) of regenerating TA muscles at day 7. Myofibre mean cross-sectional area (**c**), number of myofibres per mm (**d**), and myofibre area dis-tribution (**e**) of TA muscles at day 7 of regeneration. Myofibre mean cross-sectional area, myofibre number, and myofibre distribution at day 7 of regeneration in EAMG R-muscles were correlated with mouse clinical score (respectively, **f**–**h**). Each symbol represents one mouse clinically sick from the EAMG mouse group. In (**b**, *bottom panels*), nuclei were stained with DAPI. In **h**, *white squares* represent the distribution of the myofibres which were smaller than 600 µm^2 and *black dots* represent the ones which were bigger than 1200 µm^2. Values represent the mean ± SEM. $p < 0.01$ (**), $p < 0.001$ (***). *Bar* 20 µm

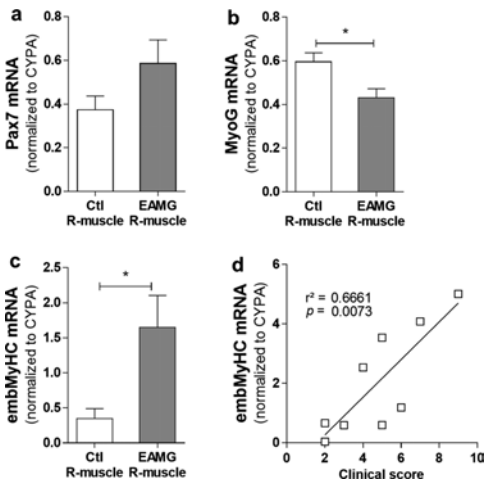

Fig. 9 EAMG regenerated muscle showed impaired regeneration compared to control regenerated muscle. Pax7 (**a**), MyoG (**b**), and embryonic MyHC (**c**) mRNA expression. Embryonic MyHC mRNA expression was correlated with the mouse clinical score (**d**). *Each symbol* represents one mouse clinically sick (score ≥2) from the EAMG mouse group. Cyclophilin A (CYPA) was used as an internal control for qPCR. Values represent the mean ± SEM. $p < 0.05$ (*)

Discussion

The purpose of this study was to characterise the functional features of SCs from MG muscle compared to the control muscle. Our main results are as follows: (1) we found an increased number of SCs associated with a high proliferative rate in the skeletal muscles of MG patients and of induced-EAMG mice compared to controls. These findings suggest that MG pathogenic mechanisms affect not only the post-synaptic membrane but also other muscle components; (2) cultured MG and control SCs from muscle biopsies displayed significant differences in proliferation and differentiation, even several weeks after being taken outside from their in vivo muscle environment; (3) cultured control SCs differentiated more rapidly when they were treated with MG sera or monoclonal anti-AChR antibodies compared to their respective controls, suggesting the implication of the circulating anti-AChR antibodies in the pathogenic mechanisms affecting the main functions of SCs; and (4) skeletal muscles of EAMG mice displayed smaller and higher number of fibres than skeletal muscles of control mice following cardiotoxin-acute injury. These findings, along with an enhanced expression of embryonic myosin heavy chain, suggest that myofibres displayed a delay of maturation during the regeneration process. Altogether, these results highlight for the first time that circulating anti-AChR autoantibodies in MG disease have pathogenic effects on SCs and muscle regeneration processes.

MG-specific factors have pathogenic effects on the number and activity of SCs

In the first part of this study, we evidenced the effects of the MG on SC quantity and activity. We showed that both MG and EAMG muscle biopsies displayed a higher number and activity of SCs than their respective controls. SCs were initially identified by electron microscopy based on their anatomical location and morphology [43]. They are essential for homoeostasis maintenance and muscle regeneration [40, 75]. SCs are able to proliferate and differentiate into skeletal muscle cells [8, 48, 64] as well as to self-renew [14, 51], which confer them the muscle stem cell grade. Dysfunction of these cells, as observed in several diseases, may cause a decrease in self-renewal with a depletion of the SC pool, whereas uncontrolled self-renewal and proliferation would result in overproduction of SCs with a tumorigenic risk [36, 62]. The observed increased number and activity of SCs in MG muscle biopsies are new information in the MG field. Many diseases affecting muscle are associated with a reduction in the SC pool [26, 29, 73]. For example, SC reduction was found in X-linked muscular dystrophy (MDX) in mice [45] or in type 1 diabetes characterised by the alteration of Notch signalling pathway on skeletal muscle [18]. On the other hand, as observed in our study, an increase in the SC pool was described in several cases such as degenerative muscle disease [34], neuromuscular disease as “arrested development of right response” (ADR) myotonia [63], drug treatment [56], or mechanical stress [11, 76]. Moreover, it is known that both number and functionality of SCs are age-dependent with a significant decline during life span until senescence [7, 74]. However, our results were carried out without any specific treatment or stress, and cells were removed from their in vivo muscle environment and from the serum pathogenic factors. In addition, they were obtained using age-matched control muscles, suggesting that the observed high number of SCs in MG biopsies was not due to an age difference. Since MyoD is known to play a critical role in the proliferation of myoblasts [62], the most likely scenario to explain the increase in the number of SCs is the increased cell activation through overexpression of MyoD, as previously seen in some neuromuscular disorders [33, 77]. This hypothesis is supported by our data showing that MG muscles displayed higher MyoD and Ki67 positive cells among total SCs compared to control muscles. Interestingly, the data from the quantitative analysis of SCs in MG muscle biopsies were supported by our ex vivo experiment using the EAMG mouse model, where an increased number of SCs were also found in *TA* muscles. Since EAMG is an induced model obtained by immunization with *Torpedo Californica* AChR, these results strongly suggest that the increased number of SCs is due to the pathogenic effects of the antibodies against AChR generated during the disease, and not to a pre-existing abnormality in MG patients. However, SCs do not express a high level of AChR. It is, therefore, very likely that the interaction of the antibodies with the AChR on the myofibres at the muscle endplate results in the production of paracrine factors, such as growth factors, microvesicles, or exosomes, which could influence the features of the SCs. An increased number of SCs could theoretically lead to muscle hypertrophy or hyperplasia. However, this was not observed in MG patients (data not shown). These data are consistent with the report of Gidaro et al. [25] that has shown that an increasing number of SCs in oculopharyngeal muscular dystrophy patient do not necessarily induce a better muscle function. This observation allows us assuming that in MG muscles, the excess of SCs could play a role in the repair of muscle fibres that have been damaged by MG pathogenic mechanisms, and this could represent a compensatory process to maintain muscle homoeostasis. This hypothesis is supported by similar observations in situations of sustained neuromuscular blockade by botulinum toxin [19]. Indeed, a single injection of Botox resulted in a significant short-term

increase in satellite cell activation and myonuclear addition in adult rabbit extraocular muscles [72].

Furthermore, our ex vivo results showed that myoblasts, from MG muscle biopsies, differentiated more rapidly than control ones. Since MyoG is known to play a role in the differentiation of myoblasts [62], we analysed the expression of this factor and showed that it was indeed more expressed in MG myoblasts compared to controls during the differentiation process. Since these effects were still observed in vitro, in the absence of paracrine factors, it is likely that intrinsic mechanisms could explain the observed high proliferation and differentiation of SCs. Moresi et al. [49, 50] have reported epigenetic changes in SCs during the myogenic processes from activation to proliferation and from proliferation to differentiation. They described the activities of the histone methylation, acetylation, and deacetylation that modulate the transcription of specific genes or the role of microRNA enhancing or repressing transcription factors during myogenesis. These data indicate a robust SC reaction in response to different types of stress. It is, therefore, likely that SCs undergo stable epigenetic changes in the MG patients that are conserved during cell culture. All together, these findings suggest that MG and control SCs display significant functional differences, raising the hypothesis that MG-specific factors are able to alter SC properties directly via paracrine factors and by acquired epigenetic modifications in SCs.

Role of anti-AChR antibodies on observed alterations of MG SC

In MG muscles, the main pathological mechanisms of anti-AChR antibodies described so far are: degradation of AChRs in a complement-dependent manner, induced AChR internalisation, and blocking of the binding site of acetylcholine to its receptor [5, 39]. These mechanisms induce a reduction in the ability of motor nerves to transmit signals thus affecting the function of the skeletal muscle [2, 3, 22]. Investigating for the first time whether the anti-AChR antibodies could induce pathogenic mechanisms that alter specifically SC features, we tested the effects of MG sera and two monoclonal AChR antibodies (mAB155 and mAB198) on the proliferation and differentiation of SCs from control muscle. Our results demonstrated that MG sera (Online Resource Fig. S2) or anti-AChR antibodies (data not shown) had no effects on the proliferation of control myoblasts, probably because of the low expression of AChR by these cells. Indeed, when expressed in myoblasts, AChRs are diffusely and weakly distributed, while when expressed in myotubes, AChRs are clustered and more largely present [42, 46]. However, the treated SCs with MG sera or mABs differentiated more rapidly than those treated with control sera or appropriate IgG control. The fact that MG sera and anti-AChR antibodies induced similar effects strongly sug-gests that the observed high differentiation is specifically mediated by anti-AChR antibodies. These results were confirmed by increased mRNA expression of the specific marker of the differentiation MyoG after the treatments. The relevance of these data is strengthened by the observation that MG muscle biopsies also displayed higher mRNA expression of MyoG compared to control ones, confirming that our in vitro model is appropriate to explore the pathogenic mechanisms in MG.

Accordingly, we assume that anti-AChR antibodies bind to the clustered and widely expressed AChRs on myofibres inducing a cascade of intracellular events and the release of factors that can affect SCs and enhance their differentiation via increase of MyoG expression. Indeed, Eftimie et al. and Asher et al. [3, 22] have demonstrated that removal or blockade of the neurotransmission signal, as well as the presence of anti-AChR antibodies, induces an increased level of MyoD and MyoG expression which in turn increase the AChR expression. This increased expression of MyoG and MyoD has also been observed when injecting in the muscle the botulinum toxin that blocks the nerve activity, suggesting that blockade of neuromuscular transmission results in a release of myogenic factors that play a major role in satellite cell function [19]. Furthermore, Maurer et al. [42] have shown that monoclonal anti-AChR antibodies induce a significant increase in IL-6 expression by control myoblasts via the modulation of Akt/mTOR signalling pathway. IL-6 is known to stimulate SC proliferation and differentiation [66]. Of note, mAB155 that is known to recognize a cytoplasmic domain was as efficient as mAB198 both for IL-6 production and myotube differentiation, raising several potential explanations: (1) mAB155 could recognize an extracellular domain in addition to its main recognition domain; (2) mAB155 could act through an FC receptor or another transporter at the muscle cell surface; and (3) if muscle cells are damaged, mAB155 could act directly on cytoplasmic domain.

Others studies support the implication of anti-AChR antibodies in the alteration of the gene transcription process on myoblasts. Indeed, Guyon et al. [27, 28] have shown in vitro, using TE671 muscle cell line and cultured normal human myotubes, a decrease in nicotinic AChR protein expression mediated by monoclonal anti-AChR antibodies. This loss induces an increase in the mRNA level of AChR subunits suggesting the presence of muscle-specific compensatory signalling pathways which regulate gene expression, to limit the loss of the AChR protein.

The reported scenarios reveal functional differences between SCs derived from control and MG muscles. We suggest that these differences may represent a pathogenic mechanism of the anti-AChR antibodies on SCs mediated by various signalling pathways that alter MyoD and MyoG expression which in turn play a key role in SC features.

Impairment of the myofibre maturation after acute injury in the EAMG mouse model

When skeletal muscle undergoes injury, satellite cells become activated and proliferate to form a pool of stem cells. Then, they differentiate and fuse to form new muscle cells. Finally, the newly formed myotubes, maturate to augment existing muscle fibres and to form new fibres. Thus the regeneration process includes three main steps: proliferation, differentiation, and maturation. Our data obtained in the EAMG model suggest that in myasthenic muscles, among all regeneration steps, the maturation process is altered. This is supported by the following experimental data: (1) we did not observe a significant difference in the expression of Pax 7, the satellite cell marker, suggesting that satellite cell proliferation is not altered; (2) we observed smaller cross-sectional area and higher number of the muscle fibres; (3) we showed an overexpression of embMyHC in myasthenic muscles compared to control ones which were correlated with the myasthenic clinical score. Thus, these data point out that during regeneration in EAMG mice, the satellite cells fuse efficiently to form small fibres, but these small fibres could not mature and fuse more to form bigger fibres.

This result could appear conflicting with our in vitro data that shows an increased differentiation by the monoclonal antibodies. Several hypotheses could be raised to explain this apparent contradiction: (1) the chronic presence of anti-AChR antibodies in the synapses of the MG mice or patients could affect the AChR permanently, interfering with the electrical signals and its numerous consequences [20, 31], while the cultures of myoblasts were not continuously treated with the anti-AChR antibodies; (2) the in vitro model is constituted of pure myoblasts and is devoid of nerve terminals and other cell types that could play a role in the maturation process. It is indeed well known that in the absence of nerve, the process of regeneration, and muscle differentiation are impaired [17].

Moreover, it is important to discuss a last point concerning the re-innervation process during muscle regeneration. Re-innervation and synapse formation are essential during skeletal muscle regeneration, especially for differentiation and maturation of myofibres [68]. Our data are the first to analyse the regeneration process after a muscle injury in the MG context. As indicated above, our data clearly show an impaired maturation process of the myofibres. It is, therefore, tempting to speculate that this defect is due to the chronic presence of anti-AChR antibodies in the synapses that could affect the re-innervation process. The arguments supporting this hypothesis are as follows: (1) in the absence of AChR, the innervation is compromised. Indeed, the clustering of the RACh in the myofibre is required for the muscle innervation [23, 52]. During the degeneration/regeneration process, the motor endplate is deprived of their post-synaptic components for a few days and the formation of the synaptic connections is impaired, since the post-synaptic folds of the skeletal neuromuscular junction contain several molecules, such as AChR, that is essential for a functional neuromuscular transmission (Reviewed in Hughes et al. [32]). However, In the EAMG model, the anti-AChR antibodies that are chronically expressed could prevent the normal expression and clustering of AChR. In this compromised situation with low AChR expression, muscle innervation is expected to be damaged. In support to these data, impaired re-innervation has already been suggested in MG patients [69]; (2) it is known that denervated muscles recover less efficiently than the non-denervated controls, following cardiotoxin injection [17]. Denervated skeletal muscle displays higher number of myofibres and higher expression of embMyHC than innervated skeletal muscles [10]. MG is a type of functional denervation as anti-AChR antibodies decrease the number of AChR, induce a simplification of the postsynaptic folds, that results in a decrease in the neuromuscular transmission [28]. Combined with our results, these literature data strongly suggest that anti-AChR antibodies may impair re-innervation of the neuromuscular junction and thereby slow down the myofiber growth.

Implication of Akt/mTOR pathway

Cohen et al. in 2015 and Bodine et al. in 2001 have discussed the fact that protein degradation could occur in muscles through genetic reduction of Akt/mTOR signalling pathway resulting in fibre atrophy [9, 12]. These data suggest that Akt/mTOR signalling pathway is a crucial regulator of muscle mass and its alteration can induce muscle atrophy in vivo. Moreover, and as we mentioned above, Maurer et al. have demonstrated that IL-6 expression, was increased in myasthenic muscles of mice [42] inducing a reduction of Akt phosphorylation and activity. Furthermore, several studies have shown that muscles of MG patients displayed muscle atrophy especially in type II fibres [41, 80].

Together, these findings suggest that anti-AChR antibodies could alter Akt/mTOR signalling pathway by modulation of IGF-1 or IL-6 expression. This alteration could explain the observed atrophy in newly regenerated myasthenic muscle fibres.

Several sports and physical practice studies have shown that a decrease in the frequency and intensity of electrical stimulation in skeletal muscle cells, as observed in MG muscles, induces defects in mTOR signalling [4, 55]. These data suggest that mTOR activity is also dependent on the neuromuscular signal transmission. On the other hand, Miyabara et al. showed that post-injury treatment of skeletal muscles with rapamycin, an mTOR signalling inhibitor, causes a delay in the expression of contractile adult MyHC and formation of newly regenerated myofibres [47]. This suggests that mTOR is critical in muscle regeneration mostly in the embryonic-to-adult MyHC shift which takes place on maturation step. Therefore, this information suggests that the observed delay of myofibre maturation in myasthenic muscles during the regeneration, evidenced by the increased expression of embryonic MyHC, could be due to a defect in the activation of the mTOR signalling. Since pAkt is known to be a downstream activator of mTOR in muscle [9], this last assumption concerning the alteration of Akt/mTOR signalling pathway could be the most likely one. Indeed, our supplemental results showed a decrease of pAkt protein expression in EAMG muscle compared to control muscle (Online Resource Fig. S7).

Conclusion

Taken together, our results led us to propose a hypothetical mechanism by which anti-AChR antibodies act. In MG muscles, we suppose that the binding of anti-AChR antibodies to the receptors on motor endplate induces molecular changes or alters the production of several paracrine factors, microvesicles or exosomes. These factors could then induce paracrine effects on the neighbouring SCs associated with subtle modifications of the epigenetic signatures. This leads to the expression of the myogenic transcription factors MyoD and MyoG in MG SCs that will proliferate and differentiate more than in healthy ones. In the case of injured MG muscles, we assume that the modulation of MyoD and MyoG expression, which could be possibly due to the alteration of Akt/mTOR signalling pathways, affects the regeneration efficiency inducing impairment of myofibre maturation. This last point is very important from the clinical point of view. The fact that clinicians know that MG muscles regenerate worse than control ones is crucial information to avoid symptom exacerbation during muscle repair following an intensive sports activity or muscle injury. Sports activity and muscle injury treatment in MG patients must, therefore, be adapted to patients and the severity of the disease. We provide here, an argument in favour of a new mechanism of action of anti-AChR antibodies on myasthenic muscles. Further experiments will be necessary to dissect the signalling pathway(s) that is (are) involved downstream the antiAChR autoantibodies impact on AChRs. The autoimmune attack in MG leads to important changes in the SC features that could represent a mechanism of compensation to preserve muscle fibres that have been damaged by the AChR autoantibodies.

Acknowledgements We thank our colleagues Jacky BISMUTH, Frédérique TRUFFAULT, Nadine DRAGIN-MAMAVI, Floriane LACOUR, Elija SCHIRWIS, Jean-Thomas VILQUIN, and all Myology Research Centre members for their valuable discussions and help. We thank all members of the SPF animal facility (CEF, Université Pierre et Marie Curie) for their valuable advice and help. We also thank our collaborator Socrates TZARTOS for his kind gift of anti-AChR monoclonal antibodies. This study was funded by a Grant from European consortium called Fight-MG (Grant Number 242210).

Compliance with ethical standards

Research involving human participants All procedures performed in studies involving human participants were in accordance with the ethical standards of the French research committee "Comité de Protection des Personnes (CPP, Ile-de-France VI)" (authorization number 2010-A00250-39) and with the 1964 Helsinki declaration and its later amendments or comparable ethical standards. All participants gave informed written consent. The experiments involving mice were performed following the principles of the French council on animal care (authorisation number: 02637).

Conflict of interest The authors declare having no conflict of interest.

References

1. Aharonov A, Tarrab-Hazdai R, Silman I, Fuchs S (1977) Immunochemical studies on acetylcholine receptor from Torpedo californica. Immunochemistry 14:129–137
2. Appel SH, Anwyl R, McAdams MW, Elias S (1977) Accelerated degradation of acetylcholine receptor from cultured rat myotubes with myasthenia gravis sera and globulins. Proc Natl Acad Sci USA 74:2130–2134
3. Asher O, Fuchs S, Zuk D, Rapaport D, Buonanno A (1992) Changes in the expression of mRNAs for myogenic factors and other muscle-specific proteins in experimental autoimmune myasthenia gravis. FEBS Lett 299:15–18
4. Baar K, Esser K (1999) Phosphorylation of p70(S6k) correlates with increased skeletal muscle mass following resistance exercise. Am J Physiol 276:C120–C127
5. Ber r ih-Aknin S, Le Panse R (2014) Myasthenia gravis: a comprehensive review of immune dysregulation and etiological mechanisms. J Autoimmun 52:90–100. doi:10.1016/j. jaut.2013.12.011
6. Ber r ih-Aknin S, Ragheb S, Le Panse R, Lisak RP (2013) Ectopic germinal centers, BAFF and anti-B-cell therapy in myasthenia gravis. Autoimmun Rev 12:885–893. doi:10.1016/j. autrev.2013.03.011
7. Bigot A, Duddy WJ, Ouandaogo ZG, Negroni E, Mariot V, Ghimbovschi S, Harmon B, Wielgosik A, Loiseau C, Devaney J, Dumonceaux J, Butler-Browne G, Mouly V, Duguez S (2015) Age-associated methylation suppresses SPRY1, leading to a failure of re-quiescence and loss of the reserve stem cell pool in elderly muscle. Cell Rep 13:1172–1182. doi:10.1016/j. celrep.2015.09.067
8. Bischoff R (1975) Regeneration of single skeletal muscle fibers in vitro. Anat Rec 182:215–235. doi:10.1002/ar.1091820207
9. Bodine SC, Stitt TN, Gonzalez M, Kline WO, Stover GL, Bauerlein R, Zlotchenko E, Scrimgeour A, Lawrence JC, Glass DJ, Yancopoulos GD (2001) Akt/mTOR pathway is a crucial regulator of skeletal muscle hypertrophy and can prevent muscle atrophy in vivo. Nat Cell Biol 3:1014–1019. doi:10.1038/ncb1101-1014
10. Carraro U, Boncompagni S, Gobbo V, Rossini K, Zampieri S, Mosole S, Ravara B, Nori A, Stramare R, Ambrosio F, Piccione F, Masiero S, Vindigni V, Gargiulo P, Protasi F, Kern H, Pond A, Marcante A (2015) Persistent muscle fiber regeneration in long term denervation past present future. Eur J Transl Myol 25:4832. doi:10.4081/ejtm.2015.4832
11. Chen JC, Goldhamer DJ (2003) Skeletal muscle stem cells. Reprod Biol Endocrinol 1:101. doi:10.1186/1477-7827-1-101
12. Cohen S, Nathan JA, Goldberg AL (2015) Muscle wasting in disease: molecular mechanisms and promising therapies. Nat Rev Drug Discov 14:58–74. doi:10.1038/nrd4467
13. Collins CA, Olsen I, Zammit PS, Heslop L, Petrie A, Partridge TA, Morgan JE (2005) Stem cell function, self-renewal, and behavioral heterogeneity of cells from the adult muscle satellite cell niche. Cell 122:289–301. doi:10.1016/j.cell.2005.05.010
14. Collins CA, Partridge TA (2005) Self-renewal of the adult skeletal muscle satellite cell. Cell Cycle 4:1338–1341
15. Conti-Fine BM, Milani M, Kaminski HJ (2006) Myasthenia gravis: past, present, and future. J Clin Investig 116:2843–2854. doi:10.1172/JCI29894
16. Couteaux R, Mira JC, d'Albis A (1988) Regeneration of muscles after cardiotoxin injury. I. Cytological aspects. Biol Cell 62:171–182
17. d'Albis A, Couteaux R, Janmot C, Roulet A, Mira JC (1988) Regeneration after cardiotoxin injury of innervated and denervated slow and fast muscles of mammals. Myosin isoform analysis. Eur J Biochem 174:103–110
18. D'Souza DM, Zhou S, Rebalka IA, MacDonald B, Moradi J, Krause MP, Al-Sajee D, Punthakee Z, Tarnopolsky MA, Hawke TJ (2016) Decreased satellite cell number and function in humans and mice with Type 1 diabetes is the result of altered notch signaling. Diabetes 65:3053–3061. doi:10.2337/ db15-1577
19. Das R, Rich J, Kim HM, McAlinden A, Thomopoulos S (2011) Effects of botulinum toxin-induced paralysis on postnatal development of the supraspinatus muscle. J Orthop Res Off Publ Orthop Res Soc 29:281–288. doi:10.1002/jor.21234
20. Drachman DB, Kao L, Angus CW, Murphy A (1977) Effect of myasthenic immunoglobulin on ACh receptors of cultured muscle. Trans Am Neurol Assoc 102:96–100
21. Edom F, Mouly V, Barbet JP, Fiszman MY, Butler-Browne GS (1994) Clones of human satellite cells can express in vitro both fast and slow myosin heavy chains. Dev Biol 164:219–229. doi:10.1006/dbio.1994.1193
22. Eftimie R, Brenner HR, Buonanno A (1991) Myogenin and MyoD join a family of skeletal muscle genes regulated by electrical activity. Proc Natl Acad Sci USA 88:1349–1353
23. Ferraro E, Molinari F, Berghella L (2012) Molecular control of neuromuscular junction development. J Cachexia Sarcopenia Muscle 3:13–23. doi:10.1007/s13539-011-0041-7
24. Garry GA, Antony ML, Garry DJ (2016) Cardiotoxin induced injury and skeletal muscle regeneration. Methods Mol Biol 1460:61–71. doi:10.1007/978-1-4939-3810-0_6
25. Gidaro T, Negroni E, Perie S, Mirabella M, Laine J, Lacau St Guily J, Butler-Browne G, Mouly V, Trollet C (2013) Atrophy, fibrosis, and increased PAX7-positive cells in pharyngeal muscles of oculopharyngeal muscular dystrophy patients. J Neuropathol Exp Neurol 72:234–243. doi:10.1097/NEN.0b013e3182854c07
26. Gnocchi VF, Scharner J, Huang Z, Brady K, Lee JS, White RB, Morgan JE, Sun YB, Ellis JA, Zammit PS (2011) Uncoordinated transcription and compromised muscle function in the lmna-null mouse model of Emery-Emery-Dreyfuss muscular dystrophy. PLoS One 6:e16651. doi:10.1371/journal.pone.0016651
27. Guyon T, Levasseur P, Truffault F, Cottin C, Gaud C, BerrihAknin S (1994) Regulation of acetylcholine receptor alpha subunit variants in human myasthenia gravis. Quantification of steady-state levels of messenger RNA in muscle biopsy using the polymerase chain reaction. J Clin Investig 94:16–24. doi:10.1172/ JCI117302
28. Guyon T, Wakkach A, Poea S, Mouly V, Klingel-Schmitt I, Levasseur P, Beeson D, Asher O, Tzartos S, Berrih-Aknin S (1998) Regulation of acetylcholine receptor gene expression in human myasthenia gravis muscles. Evidences for a compensatory mechanism triggered by receptor loss. J Clin Investig 102:249–263. doi:10.1172/JCI1248

29. He WA, Berardi E, Cardillo VM, Acharyya S, Aulino P, ThomasAhner J, Wang J, Bloomston M, Muscarella P, Nau P, Shah N, Butchbach ME, Ladner K, Adamo S, Rudnicki MA, Keller C, Coletti D, Montanaro F, Guttridge DC (2013) NF-kappaBmediated Pax7 dysregulation in the muscle microenvironment promotes cancer cachexia. J Clin Investig 123:4821–4835. doi:10.1172/JCI68523
30. Hoch W, McConville J, Helms S, Newsom-Davis J, Melms A, Vincent A (2001) Auto-antibodies to the receptor tyrosine kinase MuSK in patients with myasthenia gravis without acetylcholine receptor antibodies. Nat Med 7:365–368. doi:10.1038/85520
31. Howard FM Jr, Lennon VA, Finley J, Matsumoto J, Elveback LR (1987) Clinical correlations of antibodies that bind, block, or modulate human acetylcholine receptors in myasthenia gravis. Ann N Y Acad Sci 505:526–538
32. Hughes BW, Kusner LL, Kaminski HJ (2006) Molecular architecture of the neuromuscular junction. Muscle Nerve 33:445–461. doi:10.1002/mus.20440
33. Ishimoto S, Goto I, Ohta M, Kuroiwa Y (1983) A quantitative study of the muscle satellite cells in various neuromuscular disorders. J Neurol Sci 62:303–314
34. Kottlors M, Kirschner J (2010) Elevated satellite cell number in Duchenne muscular dystrophy. Cell Tissue Res 340:541–548. doi:10.1007/s00441-010-0976-6
35. Kramer C, Zoubaa S, Kretschmer A, Jordan D, Blobner M, Fink H (2017) Denervation versus preand postsynaptic muscle immobilization: effects On acetylcholineand musclespecific tyrosine kinase receptors. Muscle Nerve 55:101–108. doi:10.1002/mus.25159
36. Kuang S, Rudnicki MA (2008) The emerging biology of satellite cells and their therapeutic potential. Trends Mol Med 14:82–91. doi:10.1016/j.molmed.2007.12.004
37. Le Grand F, Rudnicki MA (2007) Skeletal muscle satellite cells and adult myogenesis. Curr Opin Cell Biol 19:628–633. doi:10.1016/j.ceb.2007.09.012
38. Le Panse R, Berrih-Aknin S (2005) Thymic myoid cells protect thymocytes from apoptosis and modulate their differentiation: implication of the ERK and Akt signaling pathways. Cell Death Differ 12:463–472. doi:10.1038/sj.cdd.4401611
39. Le Panse R, Berrih-Aknin S (2013) Autoimmune myasthenia gravis: autoantibody mechanisms and new developments on immune regulation. Curr Opin Neurol 26:569–576. doi:10.1097/ WCO.0b013e328364d6cd
40. Lepper C, Partridge TA, Fan CM (2011) An absolute requirement for Pax7-positive satellite cells in acute injury-induced skeletal muscle regeneration. Development 138:3639–3646. doi:10.1242/dev.067595
41. Martignago S, Fanin M, Albertini E, Pegoraro E, Angelini C (2009) Muscle histopathology in myasthenia gravis with antibodies against MuSK and AChR. Neuropathol Appl Neurobiol 35:103–110. doi:10.1111/j.1365-2990.2008.00965.x
42. Maurer M, Bougoin S, Feferman T, Frenkian M, Bismuth J, Mouly V, Clairac G, Tzartos S, Fadel E, Eymard B, Fuchs S, Souroujon MC, Berrih-Aknin S (2015) IL-6 and Akt are involved in muscular pathogenesis in myasthenia gravis. Acta Neuropathol Commun 3:1. doi:10.1186/s40478-014-0179-6
43. Mauro A (1961) Satellite cell of skeletal muscle fibers. J Biophys Biochem Cytol 9:493–495
44. Meinen S, Lin S, Ruegg MA, Punga AR (2012) Fatigue and muscle atrophy in a mouse model of myasthenia gravis is paralleled by loss of sarcolemmal nNOS. PLoS One 7:e44148. doi:10.1371/journal.pone.0044148
45. Menke A, Jockusch H (1991) Decreased osmotic stability of dystrophin-less muscle cells from the mdx mouse. Nature 349:69–71. doi:10.1038/349069a0
46. Merlie JP, Sanes JR (1985) Concentration of acetylcholine receptor mRNA in synaptic regions of adult muscle fibres. Nature 317:66–68
47. Miyabara EH, Conte TC, Silva MT, Baptista IL, Bueno C Jr, Fiamoncini J, Lambertucci RH, Serra CS, Brum PC, PithonCuri T, Curi R, Aoki MS, Oliveira AC, Moriscot AS (2010) Mammalian target of rapamycin complex 1 is involved in differentiation of regenerating myofibers in vivo. Muscle Nerve 42:778–787. doi:10.1002/mus.21754
48. Montarras D, Morgan J, Collins C, Relaix F, Zaffran S, Cumano A, Partridge T, Buckingham M (2005) Direct isolation of satellite cells for skeletal muscle regeneration. Science 309:2064–2067. doi:10.1126/science.1114758
49. Moresi V, Marroncelli N, Adamo S (2015) New insights into the epigenetic control of satellite cells. World J Stem Cells 7:945–955. doi:10.4252/wjsc.v7.i6.945
50. Moresi V, Marroncelli N, Coletti D, Adamo S (2015) Regulation of skeletal muscle development and homeostasis by gene imprinting, histone acetylation and microRNA. Biochim Biophys Acta 1849:309–316. doi:10.1016/j.bbagrm.2015.01.002
51. Moss FP, Leblond CP (1971) Satellite cells as the source of nuclei in muscles of growing rats. Anat Rec 170:421–435. doi:10.1002/ ar.1091700405
52. Mott M, Luna VM, Park JY, Downes GB, Epley K, Ono F (2017) Expressing acetylcholine receptors after innervation suppresses spontaneous vesicle release and causes muscle fatigue. Sci Rep 7:1674. doi:10.1038/s41598-017-01900-3
53. Neal A, Boldrin L, Morgan JE (2012) The satellite cell in male and female, developing and adult mouse muscle: distinct stem cells for growth and regeneration. PLoS One 7:e37950. doi:10.1371/ journal.pone.0037950
54. Oertel G (1988) Morphometric analysis of normal skeletal muscles in infancy, childhood and adolescence. An autopsy study. J Neurol Sci 88:303–313
55. Ogasawara R, Sato K, Matsutani K, Nakazato K, Fujita S (2014) The order of concurrent endurance and resistance exercise modifies mTOR signaling and protein synthesis in rat skeletal muscle. Am J Physiol Endocrinol Metab 306:E1155–E1162. doi:10.1152/ ajpendo.00647.2013
56. Oishi Y, Tsukamoto H, Yokokawa T, Hirotsu K, Shimazu M, Uchida K, Tomi H, Higashida K, Iwanaka N, Hashimoto T (2015) Mixed lactate and caffeine compound increases satellite cell activity and anabolic signals for muscle hypertrophy. J Appl Physiol 1985 118:742–749. doi:10.1152/japplphysiol.00054.2014
57. Pagala MK, Nandakumar NV, Venkatachari SA, Ravindran K, Namba T, Grob D (1990) Responses of intercostal muscle biopsies from normal subjects and patients with myasthenia gravis. Muscle Nerve 13:1012–1022. doi:10.1002/mus.880131103
58. Pevzner A, Schoser B, Peters K, Cosma NC, Karakatsani A, Schalke B, Melms A, Kroger S (2012) Anti-LRP4 autoantibodies in AChRand MuSK-antibody-negative myasthenia gravis. J Neurol 259:427–435. doi:10.1007/s00415-011-6194-7

59. Poea-Guyon S, Christadoss P, Le Panse R, Guyon T, De Baets M, Wakkach A, Bidault J, Tzartos S, Berrih-Aknin S (2005) Effects of cytokines on acetylcholine receptor expression: implications for myasthenia gravis. J Immunol 174:5941–5949
60. Rasband W (1997–2009) Image J. US National Institutes of Health, Bethesda, Maryland, USA http://rsb.info.nih.gov/ij/
61. Relaix F, Zammit PS (2012) Satellite cells are essential for skeletal muscle regeneration: the cell on the edge returns centre stage. Development 139:2845–2856. doi:10.1242/dev.069088
62. Rudnicki MA, Le Grand F, McKinnell I, Kuang S (2008) The molecular regulation of muscle stem cell function. Cold Spring Harb Symp Quant Biol 73:323–331. doi:10.1101/sqb.2008.73.064
63. Schimmelpfeng J, Jockusch H, Heimann P (1987) Increased density of satellite cells in the absence of fibre degeneration in muscle of myotonic mice. Cell Tissue Res 249:351–357
64. Seale P, Asakura A, Rudnicki MA (2001) The potential of muscle stem cells. Dev Cell 1:333–342
65. Seale P, Sabourin LA, Girgis-Gabardo A, Mansouri A, Gruss P, Rudnicki MA (2000) Pax7 is required for the specification of myogenic satellite cells. Cell 102:777–786
66. Serrano AL, Baeza-Raja B, Perdiguero E, Jardi M, Munoz-Canoves P (2008) Interleukin-6 is an essential regulator of satellite cell-mediated skeletal muscle hypertrophy. Cell Metab 7:33–44. doi:10.1016/j.cmet.2007.11.011
67. Slomic A, Rosenfalck A, Buchthal F (1968) Electrical and mechanical responses of normal and myasthenic muscle. Brain Res 10:1–78
68. Strochlic L, Cartaud A, Mejat A, Grailhe R, Schaeffer L, Changeux JP, Cartaud J (2004) 14-3-3 gamma associates with muscle specific kinase and regulates synaptic gene transcription at vertebrate neuromuscular synapse. Proc Natl Acad Sci USA 101:18189–18194. doi:10.1073/pnas.0406905102
69. Trontelj JV, Stalberg EV (1995) Multiple innervation of muscle fibers in myasthenia gravis. Muscle Nerve 18:224–228. doi:10.1002/mus.880180212
70. Tuzun E, Berrih-Aknin S, Brenner T, Kusner LL, Le Panse R, Yang H, Tzartos S, Christadoss P (2015) Guidelines for standard preclinical experiments in the mouse model of myasthenia gravis induced by acetylcholine receptor immunization. Exp Neurol 270:11–17. doi:10.1016/j.expneurol.2015.02.009
71. Tzartos SJ, Barkas T, Cung MT, Mamalaki A, Marraud M, Orlewski P, Papanastasiou D, Sakarellos C, Sakarellos-Daitsiotis M, Tsantili P, Tsikaris V (1998) Anatomy of the antigenic structure of a large membrane autoantigen, the muscle-type nicotinic acetylcholine receptor. Immunol Rev 163:89–120
72. Ugalde I, Christiansen SP, McLoon LK (2005) Botulinum toxin treatment of extraocular muscles in rabbits results in increased myofiber remodeling. Invest Ophthalmol Vis Sci 46:4114–4120. doi:10.1167/iovs.05-0549
73. Verdijk LB, Dirks ML, Snijders T, Prompers JJ, Beelen M, Jonkers RA, Thijssen DH, Hopman MT, Van Loon LJ (2012) Reduced satellite cell numbers with spinal cord injury and aging in humans. Med Sci Sports Exerc 44:2322–2330. doi:10.1249/ MSS.0b013e3182667c2e
74. Verdijk LB, Snijders T, Drost M, Delhaas T, Kadi F, van Loon LJ (2014) Satellite cells in human skeletal muscle; from birth to old age. Age (Dordr) 36:545–547. doi:10.1007/s11357-013-9583-2
75. von Maltzahn J, Jones AE, Parks RJ, Rudnicki MA (2013) Pax7 is critical for the normal function of satellite cells in adult skeletal muscle. Proc Natl Acad Sci USA 110:16474–16479. doi:10.1073/pnas.1307680110
76. Wang JH, Thampatty BP (2006) An introductory review of cell mechanobiology. Biomech Model Mechanobiol 5:1–16. doi:10.1007/s10237-005-0012-z
77. Wanschitz JV, Dubourg O, Lacene E, Fischer MB, Hoftberger R, Budka H, Romero NB, Eymard B, Herson S, Butler-Browne GS, Voit T, Benveniste O (2013) Expression of myogenic regulatory factors and myo-endothelial remodeling in sporadic inclusion body myositis. Neuromuscul Disord 23:75–83. doi:10.1016/j. nmd.2012.09.003
78. Weiss JM, Robinet M, Aricha R, Cufi P, Villeret B, Lantner F, Shachar I, Fuchs S, Souroujon MC, Berrih-Aknin S, Le Panse R (2016) Novel CXCL13 transgenic mouse: inflammation drives pathogenic effect of CXCL13 in experimental myasthenia gravis. Oncotarget 7:7550–7562. doi:10.18632/oncotarget.6885
79. Yin H, Price F, Rudnicki MA (2013) Satellite cells and the muscle stem cell niche. Physiol Rev 93:23–67. doi:10.1152/ physrev.00043.2011
80. Zamecnik J, Vesely D, Jakubicka B, Cibula A, Pitha J, Schutzner J, Mazanec R (2009) Atrophy of type II fibres in myasthenia gravis muscle in thymectomized patients: steroid-induced change with prognostic impact. J Cell Mol Med 13:2008–2018. doi:10.1111/j.1582-4934.2008.00431.x
81. Zammit PS, Relaix F, Nagata Y, Ruiz AP, Collins CA, Partridge TA, Beauchamp JR (2006) Pax7 and myogenic progression in skeletal muscle satellite cells. J Cell Sci 119:1824–1832. doi:10.1242/jcs.02908
82. Zhang B, Tzartos JS, Belimezi M, Ragheb S, Bealmear B, Lewis RA, Xiong WC, Lisak RP, Tzartos SJ, Mei L (2012) Autoantibodies to lipoprotein-related protein 4 in patients with double-seronegative myasthenia gravis. Arch Neurol 69:445–451. doi:10.1001/ archneurol.2011.2393
83. Zouvelou V, Rentzos M, Toulas P, Evdokimidis I (2012) AchR-positive myasthenia gravis with MRI evidence of early muscle atrophy. J Clin Neurosci 19:918–919. doi:10.1016/j. jocn.2011.09.022

Supplemental data

	Patient number	Gender	Age (years)	Application
Control				
	CTRL1	F	56	Histology
	CTRL2	M	44	Histology
	CTRL3	M	35	Histology
	CTRL4	M	47	Histology
	CTRL5	M	39	Histology and qPCR
	CTRL6	M	40	qPCR
	CTRL7	F	44	qPCR
	CTRL8	M	53	qPCR
	CTRL9	M	30	qPCR
	CTRL10	F	22	qPCR
	CTRL11	M	44	qPCR
	CTRL12	M	44	qPCR
	CTRL13	M	40	qPCR
	CTRL14	M	30	SCs isolation
	CTRL15	M	44	SCs isolation
	CTRL16	M	47	SCs isolation
	CTRL17	F	49	SCs isolation
	CTRL18	M	48	SCs isolation
	CTRL19	M	21	SCs isolation

N/A = not applicable, F = female, M = male, SCs = satellite cells, qPCR = quantitative Polymerase Chain Reaction

Table.S1a Patient's information of control muscle biopsies. N/A = not applicable, F = female, M = male, SCs = satellite cells, qPCR = quantitative Polymerase Chain Reaction

	Patient number	Gender	Age (years)	AChR antibody (nmol/L)	Thymus histology	MG Onset age	MG grade	Treatment	Application
MG									
	MG1	F	36	> 100	Normal	32	IIa	Mytelase	Histology
	MG2	F	40	> 100	Hyperplasia	18	IVb	Mestinon	Histology
	MG3	F	28	278	Hyperplasia	28	Ia	Mestinon	Histology
	MG4	F	33	> 100	Normal	32	IIIb	Mestinon, IgG	Histology
	MG5	F	34	101	Normal	19	IIb	Mestinon	Histology and qPCR
	MG6	F	29	3.36	Hyperplasia	20	IIa	Mestinon	qPCR
	MG7	F	24	130	Hyperplasia	14	IIIa	Mestinon	qPCR
	MG8	F	28	278	Hyperplasia	20	Ia	Mestinon	qPCR
	MG9	F	20	39.74	Hyperplasia	20	IIIb	Mytelase	qPCR
	MG10	M	27	15	Thymoma	27	IIb	Mytelase	qPCR
	MG11	M	35	31.2	Thymoma	35	IIa	Mytelase	qPCR
	MG12	M	31	> 18.8	Thymoma	31	IIb	Mestinon, Mytelase	qPCR
	MG13	M	30	> 14	Hyperplasia	29	IIb	Mestinon	qPCR
	MG14	M	36	29	Hyperplasia	34	IIb	Mestinon, Mytelase	qPCR
	MG15	M	25	> 100	Thymoma	25	U/K	Mestinon	SCs isolation
	MG16	F	40	> 100	Hyperplasia	18	IVb	Mestinon	SCs isolation
	MG17	F	33	> 100	Hyperplasia	32	IIIb	Mestinon	SCs isolation
	MG18	F	28	> 100	Hyperplasia	26	IIb	Mestinon	SCs isolation
	MG19	F	51	27.5	Normal	U/K	U/K	Mestinon	SCs isolation
	MG20	F	34	11.9	Hyperplasia	34	I	Mestinon	SCs isolation

MG = Myasthenia Gravis patient, U/K = unknown, F = female, M = male, SCs = satellite cells, qPCR = quantitative Polymerase Chain Reaction, MG grade = stage of MG indexed from class I to class V according to the Myasthenia Gravis Foundation of America, Inc. (MGFA)

Table.S1b Patient's information of myasthenic muscle biopsies. U/K = Unknown, F = female, M = male, SCs = satellite cells, qPCR = quantitative Polymerase Chain Reaction, IgG = Immunoglobulin G. MG grade is the severity of MG indexed from class I to class V according to the Myasthenia Gravis Foundation of America Inc. (MGFA). Mestinon and Mytelase are an acetylcholinesterase inhibitors.

Genes	Primers	Anealing temperature (° C)	Cycles	Product size (bp)
Human Pax7	5' -GTTTGCCCCACAGACAAGAT-3' (forward) 5' -TGGAAGGAACTGGTGGTC- 3' (reverse)	60	45	237
Human MyoD	5' -CACTCCGGTCCCAAATGTAG-3' (forward) 5-'GCTCTGGCAAAGCAACTCTT-3' (reverse)	60	40	124
Human MyoG	5' -GGGAACCTTCCAGTGGTTTT-3' (forward) 5' -AAGAAATCACCCCCAAGAGG-3' (reverse)	62	45	139
Human Myf5	5' -GCTCATCAAAATGTCTCTGGTG-3' (forward) 5' -TTCTTATATCTTGAAATGATCCACAA-3' (reverse)	62	40	250
Human Emerin	5' -CAGAGTAGTGCTTGCTCCCC-3' (forward) 5' -ACAAAGTCAGGGTGGCCTTT-3' (reverse)	60	40	152
Mouse Pax7	5' -GGGCTCTTCAAGGTCTGGAC-3' (forward) 5' -CAGGGAGCAAGGAATGTGGA-3' (reverse)	62	45	136
Mouse MyoG	5'-GGGCAAACTCAGGAGCTTCT-3' (forward) 5'-CAGAGGCTTTGGAACCGGAT-3' (reverse)	62	45	211
Mouse embryonic MyHC	5'-AAGGCCAAAAAGGCCATC-3' (forward) 5'-TCTTCTGCTCCCCTTCCA-3' (reverse)	62	45	235
Mouse Cyclophilin A (PPIA)	5'-AAGAAGATCACCATTTCCGACT-3' (forward) 5'-TTACAGGACATTGCGAGC-3' (reverse)	60	40	129

Table.S2 qPCR primer sequences details

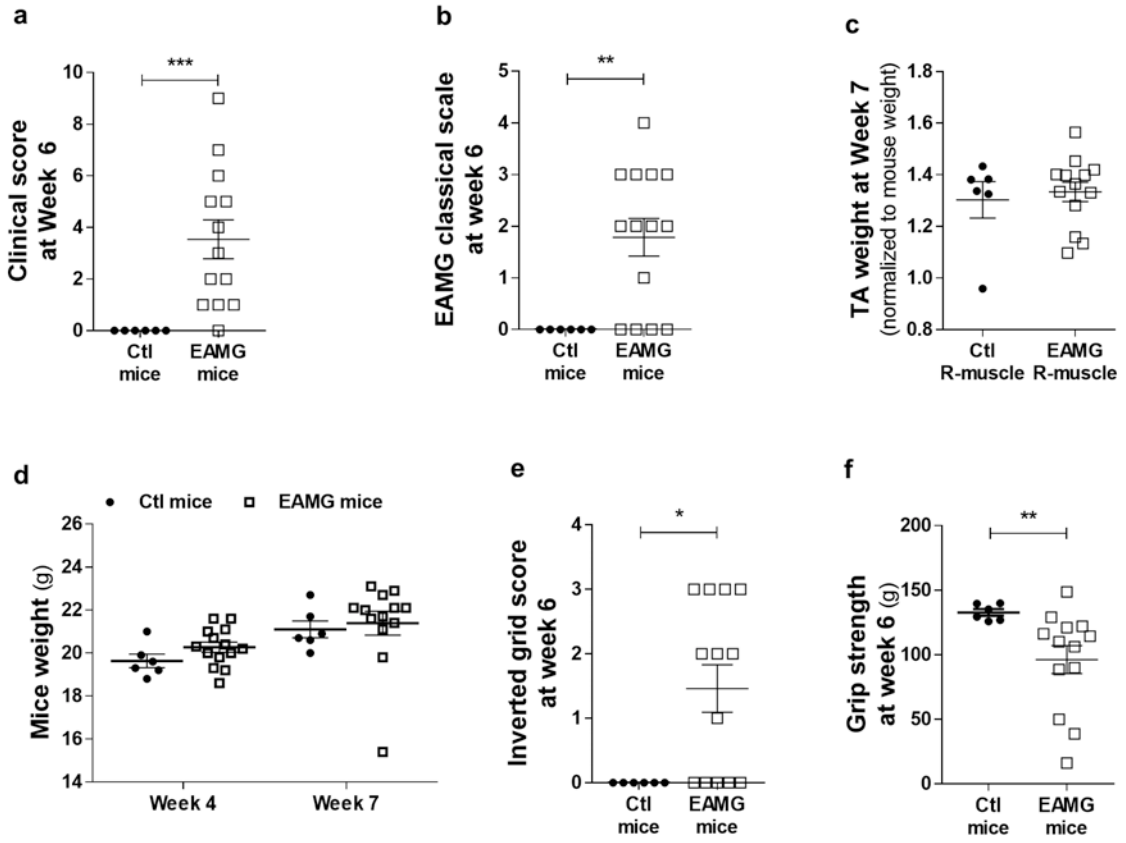

Fig.S1 Purified-AChR injections in mice induced MG symptoms evaluated by body weight, grid score and grip strength. Clinical score (a) and EAMG classical scale (b) of control (n=6) and EAMG (n=13) mice at week 6 post-immunization. Clinical score was calculated as described in Materials and Methods section. EAMG classical scale was performed according to the scale of Tuzun, E. *et al*. (Exp. Neurol, 2015). Weight of regenerated right TA muscle of control and EAMG mice at week 7 (day of sacrifice and sampling) (c). Body weight of control and EAMG injected mice at week 4 (boost of the immunization) and week 7 (day of sacrifice and muscle sampling) (d). Inverted grid score (e) and grip strength values (f) of control and EAMG mice before cardiotoxin-induced muscle regeneration. Values represent the mean ± SEM. $p < 0.001$ (***)

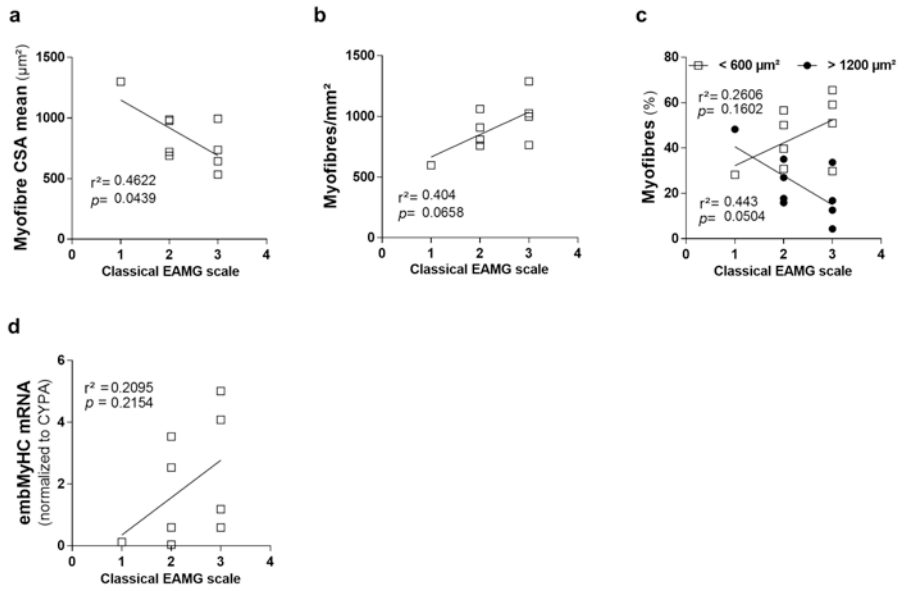

Fig.S2 Individual items and linear regression were recalculated using the EAMG classical scale. Correlation of myofibre CSA mean (a), myofibre number (b), myofibre distribution (d) and embMyHC mRNA expression with the EAMG classical scale. Each symbol represents one mouse clinically sick (score ≥ 1) from the EAMG mouse group. Cyclophilin A (CYPA) was used as an internal control for qPCR. Values represent the mean ± SEM.

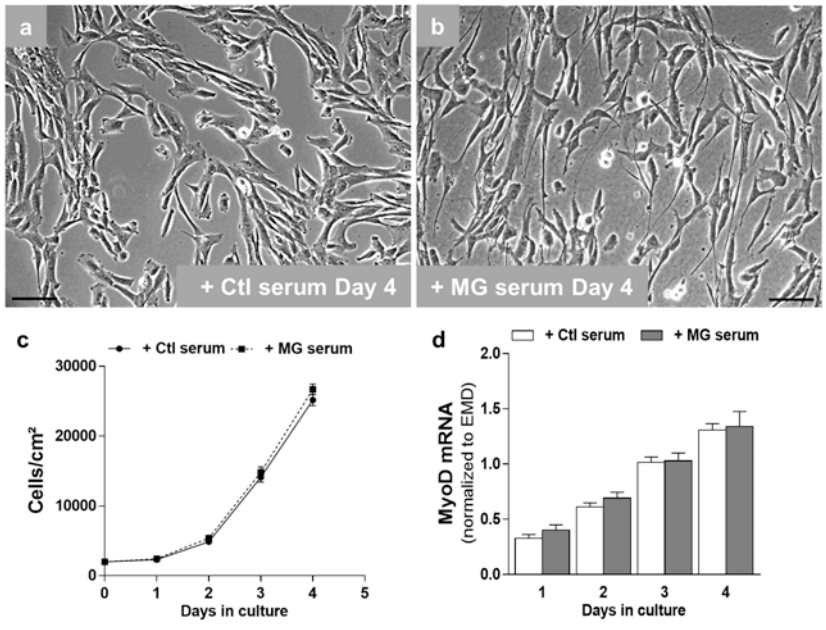

Fig.S3 MG sera treatment had no effect on the proliferation of control myoblast. Myoblasts from control muscle biopsies (n=6) were allowed to proliferate in a kinetic study (Day 0 to Day 4) in growth medium supplemented with Ctl (n=3) or MG (n=6) sera. Phase-contrast microscopy views of control myoblasts at Day 4 of proliferation treated with Ctl (a) or MG (b) sera and cell density quantification (c). MyoD mRNA level expression (d) during the proliferation. Emerin (EMD) was used as an internal control for qPCR. Values represent the mean ± SEM. Bar = 50 µm

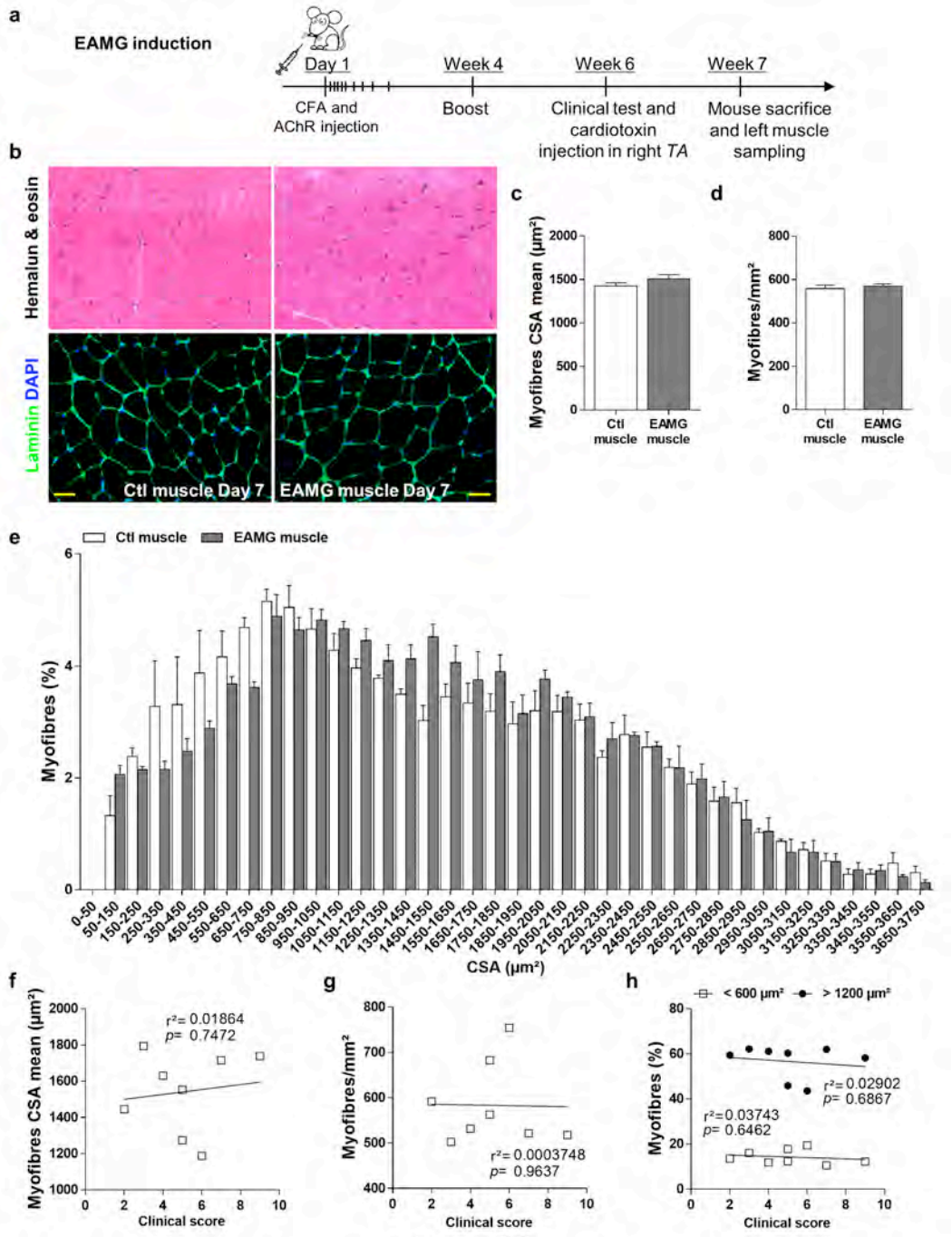

Fig.S4 Non-regenerating TA muscles of control mice displayed no differences compared to muscles of EAMG mice. Experimental design (a): Six-weeks-old female randomised-mice were injected subcutaneously at Day 1 with CFA (n=6) or CFA+AChR (n=13) to induce EAMG. At Week 7, left TA contralateral muscles (Control and EAMG muscle) which were not injected with cardiotoxin were sampled then analysed. Haematoxylin & eosin staining (b, upper panels) and Laminin immunolabeling (b, bottom panels) of contralateral TA muscles. Myofibre mean cross sectional area (c), number of myofibres per mm² (d) and myofibre area distribution (e) of control and EAMG muscles (upper panel). Myofibre mean cross-sectional area, myofibre number and myofibre distribution of EAMG muscle were not correlated with mouse clinical score (respectively f, g and h). Each symbol represents one mouse clinically sick from the EAMG mouse group. In (b, bottom panels) nuclei were stained with DAPI. In (h), white squares represent distribution of the myofibres which are smaller than 600 µm² and black dots represent the ones which are bigger than 1200 µm². Values represent the mean ± SEM. Bar = 20 µm

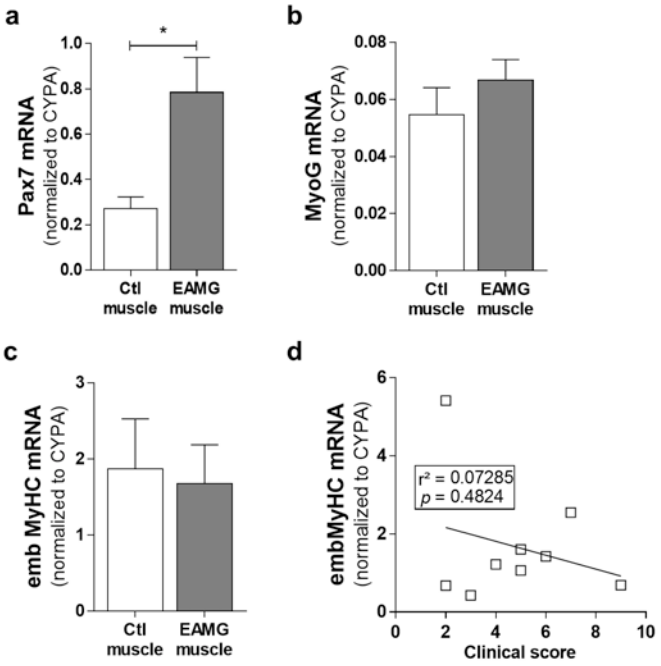

Fig.S5 mRNA expressions of MyoG and embryonic MyHC were not modulated in contralateral EAMG muscle. Pax7 (a), MyoG (b) and embryonic MyHC (c) mRNA expression. Embryonic MyHC mRNA expression was not correlated with the mouse clinical score (d). Each symbol represents one mouse clinically sick (score ≥ 2) from the EAMG mouse group. Cyclophilin A (CYPA) was used as an internal control for qPCR. Values represent the mean ± SEM. $p < 0.05$ (*)

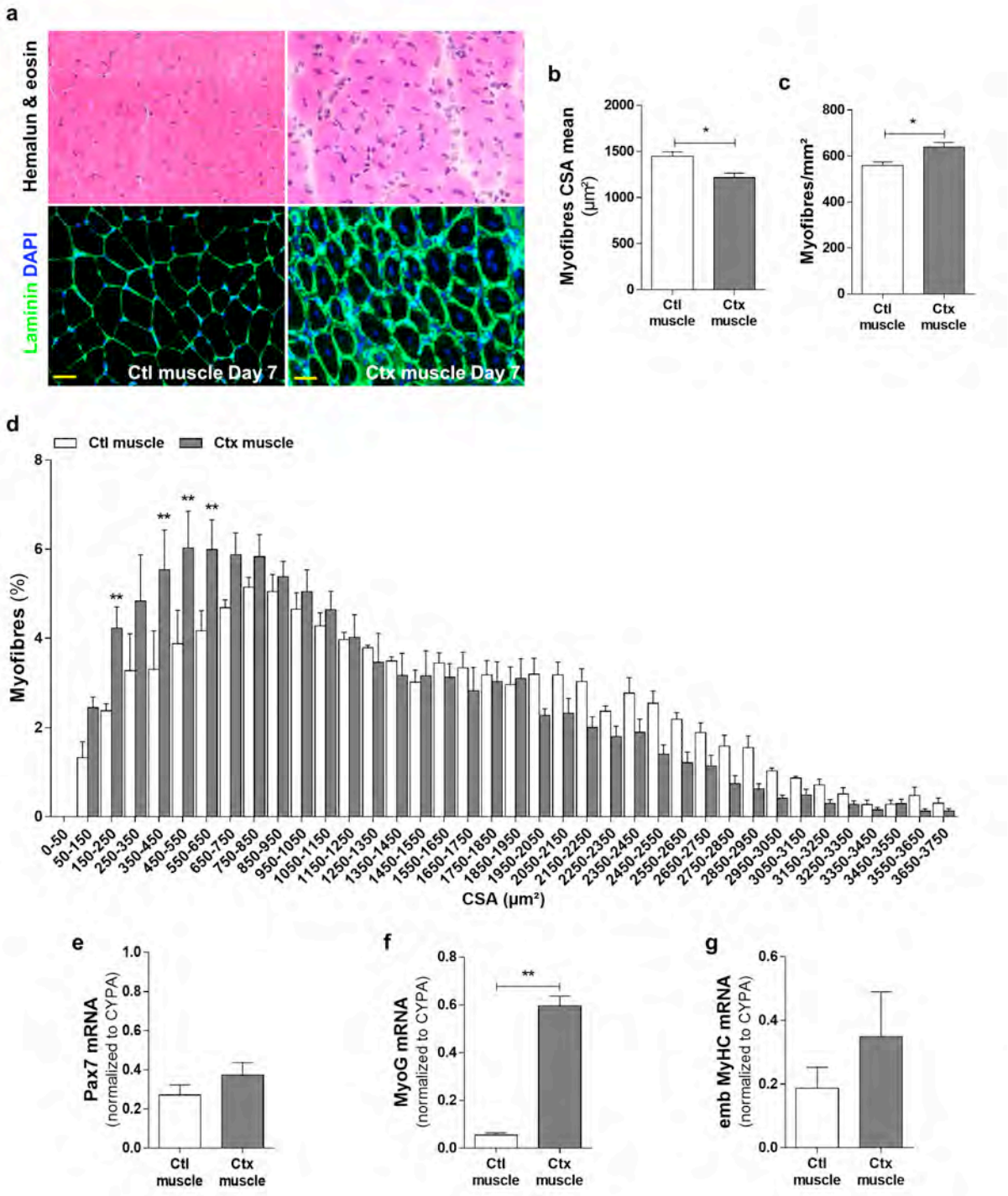

Fig.S6 Effects of cardiotoxin injection on TA muscles of control mice. Six-weeks-old female randomised-mice, from CFA group, were injected intramuscularly with cardiotoxin at Week 6 of EAMG protocol. At Week 7, contralateral (n=5, Ctl muscle) and cardiotoxin-injected (n=6, Ctx muscle) TA muscles were sampled then analysed. Haematoxylin & eosin staining (a, upper panels) and Laminin immunolabeling (a, bottom panels) of contralateral (left panels) and cardiotoxin-injected (right panels) TA muscles. Myofibre mean cross sectional area (b), number of myofibres per mm² (c) and myofibre area distribution (d) of contralateral and cardiotoxin-injected TA muscles. Pax7 (e), MyoG (f) and embryonic MyHC (g) mRNA expression in Ctl muscle and Ctx muscle. In (a, bottom panels) nuclei were stained with DAPI. Values represent the mean ± SEM. Bar = 20 µm

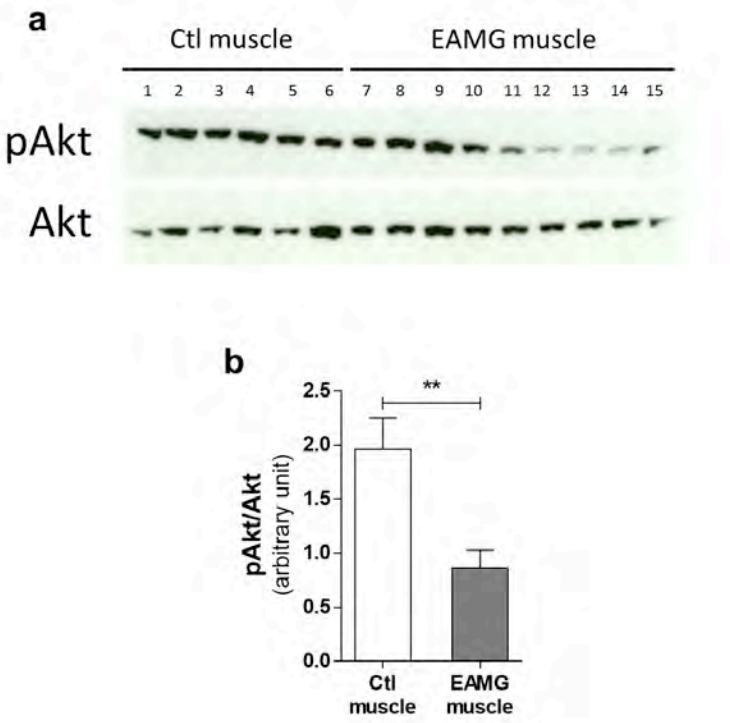

Fig.S7 The Akt/mTOR signalling pathway was altered in EAMG skeletal muscle. pAkt is known to have an important downstream effects on the activation of mTOR. Total proteins of CFA and EAMG-sicked mice were extracted from *tibialis anterior* and analysed by Western Blot. A representative image of the Western Blot result of pAkt and total Akt is shown in panel (a). The quantification of pAkt normalized to total Akt is represented in graph (b). Values represents the mean ± SEM. $p < 0.01$ *(**)*